

As a library, NLM provides access to scientific literature. Inclusion in an NLM database does not imply endorsement of, or agreement with, the contents by NLM or the National Institutes of Health.

Learn more: [PMC Disclaimer](#) | [PMC Copyright Notice](#)



Plant Physiol. 2016 Apr 4;171(2):833–848. doi: [10.1104/pp.16.00173](https://doi.org/10.1104/pp.16.00173)

Pectin Methylesterification Impacts the Relationship between Photosynthesis and Plant Growth¹ [\[OPEN\]](#)

[Sarathi M Weraduwege](#)^{1,2,3}, [Sang-Jin Kim](#)^{1,2,3}, [Luciana Renna](#)^{1,2,3}, [Fransisca C Anozie](#)^{1,2,3,✉}, [Thomas D Sharkey](#)^{1,2,3,*}, [Federica Brandizzi](#)^{1,2,3,*}

[Author information](#) [Article notes](#) [Copyright and License information](#)

PMCID: PMC4902601 PMID: [27208234](#)

High levels of methylesterification of pectin allow for enhanced cell expansion, partitioning of resources to leaf growth, and increased leaf area for photosynthesis, which in turn enhance plant growth.

Abstract

Photosynthesis occurs in mesophyll cells of specialized organs such as leaves. The rigid cell wall encapsulating photosynthetic cells controls the expansion and distribution of cells within photosynthetic tissues. The relationship between photosynthesis and plant growth is affected by leaf area. However, the underlying genetic mechanisms affecting carbon partitioning to different aspects of leaf growth are not known. To fill this gap, we analyzed Arabidopsis plants with altered levels of pectin methylesterification, which is known to modulate cell wall plasticity and plant growth. Pectin methylesterification levels were varied through manipulation of *cotton Golgi-related (CGR) 2* or *3* genes encoding two functionally redundant pectin methyltransferases. Increased levels of methylesterification in a line over-expressing *CGR2* (*CGR2OX*) resulted in highly expanded leaves with enhanced intercellular air spaces; reduced methylesterification in a mutant lacking both *CGR*-genes 2 and 3 (*cgr2/3*) resulted in thin but dense leaf mesophyll that

limited CO₂ diffusion to chloroplasts. Leaf, root, and plant dry weight were enhanced in *CGR2OX* but decreased in *cgr2/3*. Differences in growth between wild type and the *CGR*-mutants can be explained by carbon partitioning but not by variations in area-based photosynthesis. Therefore, photosynthesis drives growth through alterations in carbon partitioning to new leaf area growth and leaf mass per unit leaf area; however, *CGR*-mediated pectin methylesterification acts as a primary factor in this relationship through modulation of the expansion and positioning of the cells in leaves, which in turn drive carbon partitioning by generating dynamic carbon demands in leaf area growth and leaf mass per unit leaf area.

Photosynthesis is the major source of carbon (C) for plant growth. However, there is no clear correlation between area-based photosynthesis and plant growth, and studies have shown that the relationship between photosynthesis and plant growth is affected by leaf area growth parameters. A strong positive correlation exists between relative growth rate and leaf growth parameters such as leaf area per unit leaf mass (specific leaf area, [SLA](#)), leaf area per unit plant mass (leaf area ratio), and investment of C in leaf growth (leaf mass ratio; [Shipley, 2002](#); [Lambers et al., 2008](#); [Poorter et al., 2009](#)). In fact, modeled partitioning coefficients obtained from the Arabidopsis leaf area growth model showed that plant growth is more sensitive to changes in C partitioning to leaf thickening and leaf area growth than to changes to area-based photosynthesis ([Weraduwaage et al., 2015](#)). The term “thickening” was used to indicate increased mass per unit leaf area ([LMA](#)), whether that results from increased thickness in the normal sense of more depth to the leaf between adaxial and abaxial surfaces or from increased cell density. [LMA](#) is the reciprocal of [SLA](#). While [LMA](#) has been shown to positively and linearly correlate with investment to leaves in the form of anatomical and chemical composition changes, [SLA](#) shows a hyperbolic relationship with such changes ([Poorter et al., 2009](#)). Therefore, we will mainly focus on [LMA](#) throughout this work. [Weraduwaage et al. \(2015\)](#) concluded that even though photosynthetic C is required for growth, the degree of growth is determined by the amount of C partitioned to leaf area growth and [LMA](#) ([Weraduwaage et al., 2015](#)). However, how and to what degree this variation in leaf expansion and [LMA](#) is affected by cell wall properties of leaf mesophyll cells is not known. In addition, the underlying mechanisms that drive C partitioning to favor either leaf area growth or [LMA](#), and the genes that can influence changes in C demands toward these two processes, are yet to be found.

Leaves are the major photosynthetic organs in plants and regulation of cell expansion and growth is crucial for the development of leaf architecture. Leaf growth can occur in the form of leaf area or [LMA](#) ([Lambers et al., 2008](#); [Weraduwaage et al., 2015](#)). The size and shape of cells in the leaf mesophyll can have a significant impact on: (1) projected or effective leaf surface area, which is the leaf area capable of intercepting light; (2) leaf mass per unit leaf area or [LMA](#); (3) CO₂ conductance from the external environment through intercellular air spaces into chloroplasts in mesophyll cells; and (4) surface area of mesophyll cells and chloroplasts exposed to intercellular airspaces ([Honda and Fisher, 1978](#); [Evans et al., 1994](#); [Galmés et al., 2013](#)). The plant cell wall controls expansion and positioning of cells of photosynthetic tissues and therefore, changes in cell wall properties will have a direct impact on the above properties. Although there is evidence for changes in leaf architecture as a result of alterations in genes that affect the synthesis and

properties of the cell wall ([Burton et al., 2000](#); [Kim and Delaney, 2002](#); [Pilling et al., 2004](#); [Wolf et al., 2009](#); [Kim et al., 2015](#)), an in-depth analysis of effects on leaf gas exchange and overall plant growth under such circumstances has not yet been conducted.

The plant cell wall is composed mainly of polysaccharides, and among these, pectin is considered a critical element that controls cell wall elasticity and expansion. Pectin is synthesized in the Golgi apparatus and secreted in a highly methylesterified form. Methylesterification of galacturonic acid (GalUA) is catalyzed by pectin methyltransferases ([Wolf et al., 2009](#); [Kim et al., 2015](#)). The level of pectin methylesterification in the cell wall is controlled by methylesterases and inhibitors of methylesterases, which modify the levels of methylation and demethylation of GalUA in the pectin backbone ([Wolf et al., 2009](#); [Kim et al., 2015](#)). Removal of methyl groups by methylesterases allows carboxyl groups of GalUA to form Ca^{2+} - and Mg^{2+} -mediated intermolecular linkages that lead to hardening of pectin ([Burton et al., 2000](#); [Heldt and Piechulla, 2010](#); [Kim et al., 2015](#)). Indeed, over-expression of pectin methylesterase inhibitors results in longer root cells ([Lionetti et al., 2007](#)). Therefore, the degree of methylation and demethylation of pectin determines the delicate balance between cell wall extensibility and rigidity with consequent effects on growth and shape of cells ([Burton et al., 2000](#); [Pilling et al., 2004](#); [Lionetti et al., 2007](#); [Wolf et al., 2009](#); [Xiao and Anderson, 2013](#); [Kim et al., 2015](#)). Consistent with this notion, over-expression of pectin methyltransferases, *CGR2* or *CGR3*, led to enhanced rosette size and fresh weight in Arabidopsis ([Kim et al., 2015](#)). However, a double knockout of *CGR2* and *CGR3* genes, named *cgr2/3*, showed reduced cell expansion and overall plant growth; both phenotypes correlated with reduced levels of pectin methylesterification compared to wild type ([Kim et al., 2015](#)). To our knowledge, the effect of pectin methylation on leaf growth parameters, photosynthesis, and respiration through its effect on leaf architecture has not been studied.

The goal of this study was to use the Arabidopsis model system developed by [Kim et al. \(2015\)](#) with altered levels of pectin methyltransferases, *CGR2* or *CGR3* (single gene modifiers found to positively or negatively affect cell expansion as a function of their cellular availability) to investigate how changes in cell-wall plasticity affect C assimilation, leaf respiration, and overall plant growth through effects on leaf area growth and mesophyll structure. We examined whether the changes in overall plant growth in Arabidopsis with altered *CGR2* and *CGR3* could result from changes in leaf area growth and [LMA](#) or changes in area-based photosynthesis to explore the relationship between photosynthesis and growth. Based on the differences in rosette size reported previously ([Kim et al., 2015](#)), we hypothesized that area-based photosynthesis rates would be lower in a *CGR2* over-expressor (*CGR2OX*) but larger in the mutant lacking both *CGR2* and *3* genes (*cgr2/3*). As *CGR2* and *CGR3* affect pectin methylation and cell expansion in leaves, we also hypothesized that plant growth would be enhanced in the *CGR2OX* line and reduced in the *cgr2/3* mutant mainly as a result of altered [LMA](#). Indeed, through analysis of leaf and plant growth, gas exchange, and growth modeling, we found that *CGR2* and *CGR3* have significant impacts on photosynthesis and respiration through alteration of mesophyll structure and [LMA](#). Plant growth was enhanced in the *CGR2OX* line but reduced in the *cgr2/3* mutant. This variation in plant growth was as a result of differences in C partitioning and not as a result of changes in photosynthetic rate per unit leaf area. These observations support a novel (to our knowledge) model that changes in cell wall plasticity due to changes in pectin

composition influence C partitioning between leaf area growth and [LMA](#), thereby regulating the relationship between photosynthesis and plant growth.

RESULTS

CGR2OX and *cgr2/3* Mutant Lines Retained Altered Cell Wall Composition

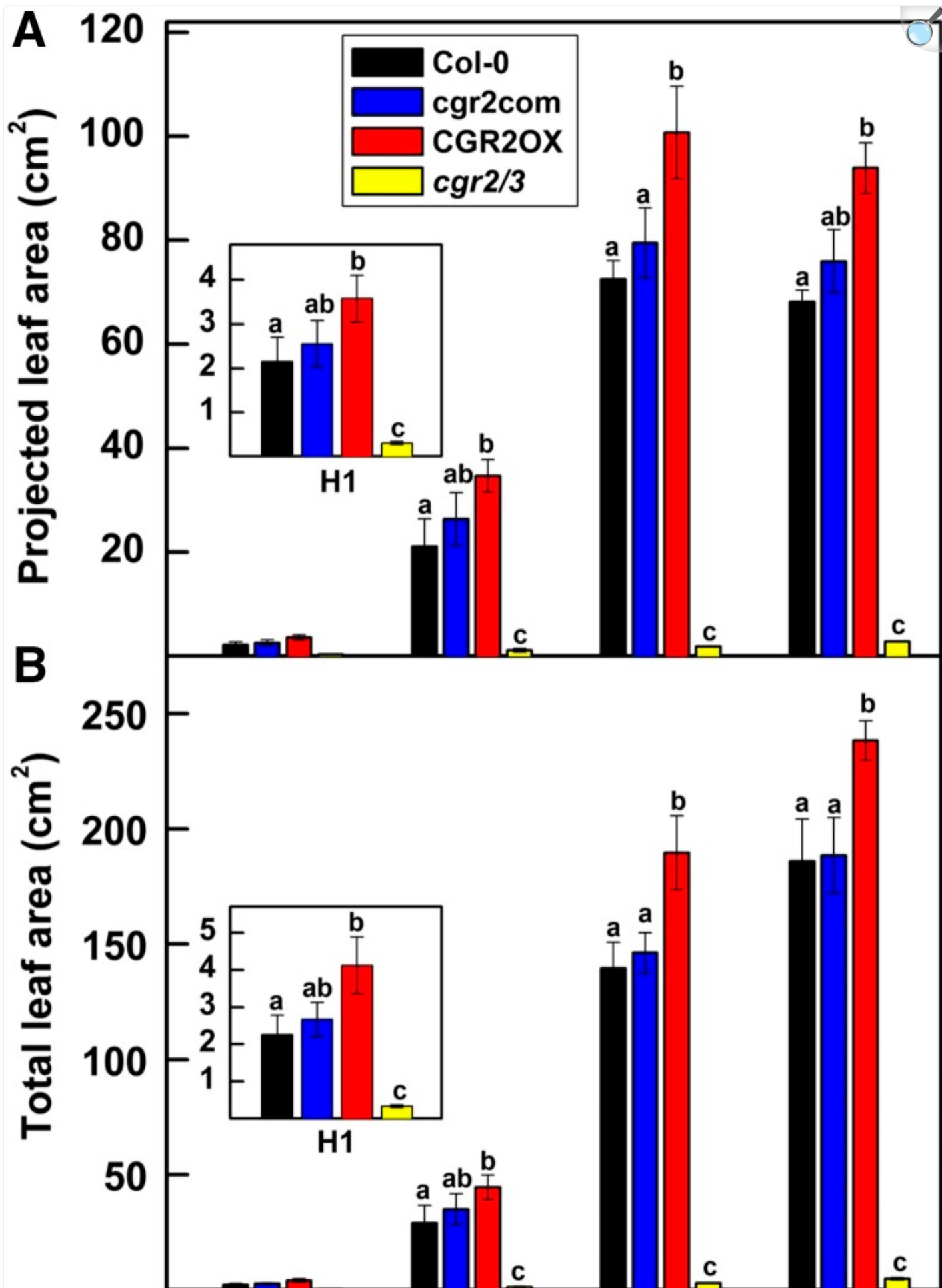
Cell wall composition of Col-0 (wild type), *cgr2/3* complemented with *CGR2* (*cgr2com*), CGR2OX, and *cgr2/3* was analyzed to determine whether the previously observed changes in methylesterification and modification of cell wall polysaccharides by [Kim et al. \(2015\)](#) were retained in the mutant lines. Similar to what was seen by [Kim et al. \(2015\)](#), crystalline cellulose content was lower in *cgr2/3* mutant line and it was greater in CGR2OX than that in Col-0 ([Supplemental Fig. S1A](#)). In addition, the content of neutral sugars such as fucose, arabinose, and glucose was significantly higher in *cgr2/3* than Col-0, as was shown by [Kim et al. \(2015\)](#); [Supplemental Fig. S1B](#)). The uronic-acid content and the amount of methylesters per uronic acid were greater in CGR2OX compared to wild type; the uronic-acid content was lower in *cgr2/3* ([Supplemental Fig. S1C](#)). These data support that the cell wall composition, including pectin and the degree of methylesterification, is altered in the CGR2OX and *cgr2/3* mutant lines in response to altered *CGR2* and *CGR3* gene expression, as previously reported in [Kim et al. \(2015\)](#).

Enhanced Pectin Methylesterification Increased Leaf Area while a Decrease in Pectin Methylesterification Reduced Leaf Area

Hypocotyl length and cotyledon and leaf areas were measured to determine how altered expression of *CGR2* and *CGR3* affects early seedling growth and expansion of the leaf blade.

Similar to earlier results ([Kim et al., 2015](#)), hypocotyls of CGR2OX were significantly longer than wild type, while those of *cgr2/3* were shorter ([Supplemental Figs. S2A](#) and [S3A](#)). Cotyledon area was also smaller in *cgr2/3* than Col-0 ([Supplemental Fig. S3B](#)). The CGR2OX mutant produced rosettes with greater projected and total leaf area compared to Col-0 throughout the lifecycle ([Fig. 1](#), [Supplemental Fig. S2, B and C](#)). In contrast, a significant reduction in projected and total leaf area was observed in *cgr2/3*. The degree of leaf overlap measured by the ratio between projected and total leaf area was not different between the transgenic lines and Col-0 ([Fig. 1](#)). Thus, functional availability of *CGR2* and *CGR3* has a significant impact on leaf area growth.

Figure 1.



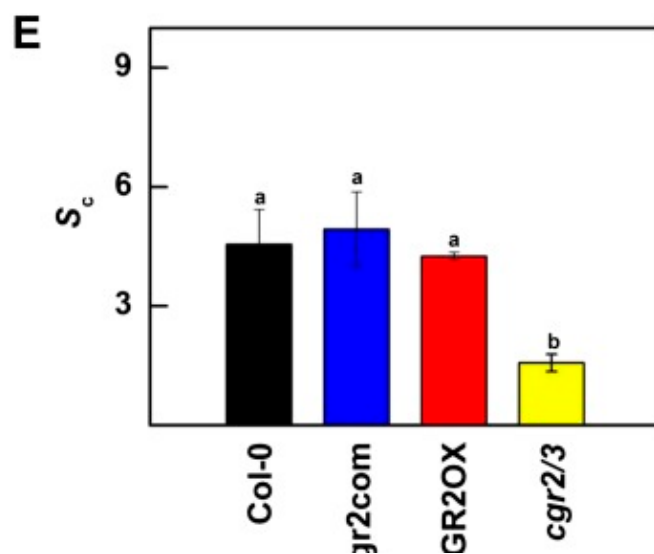
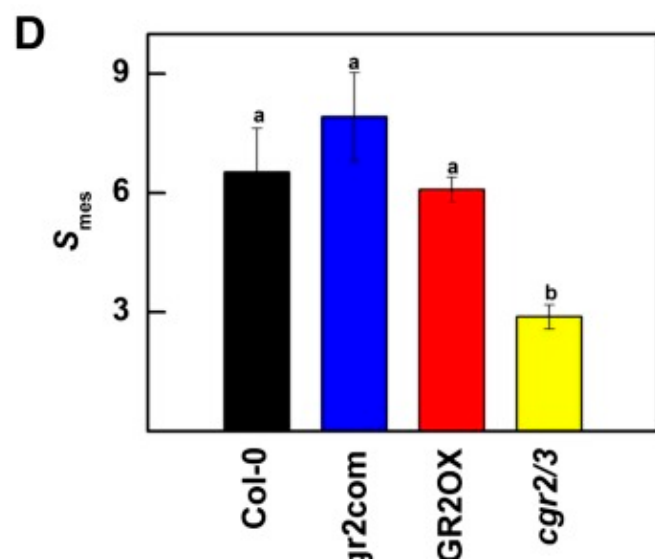
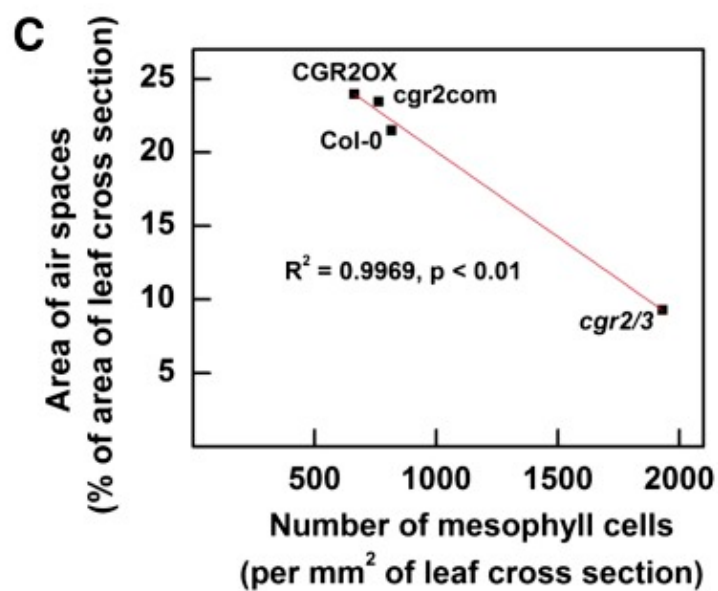
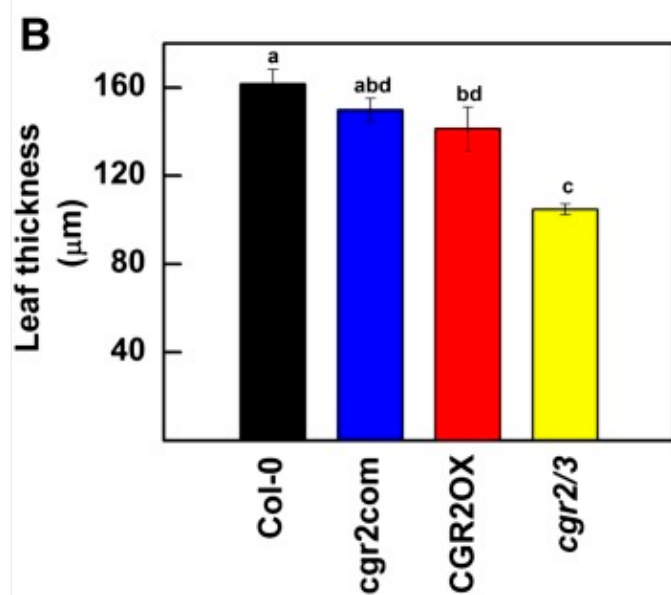
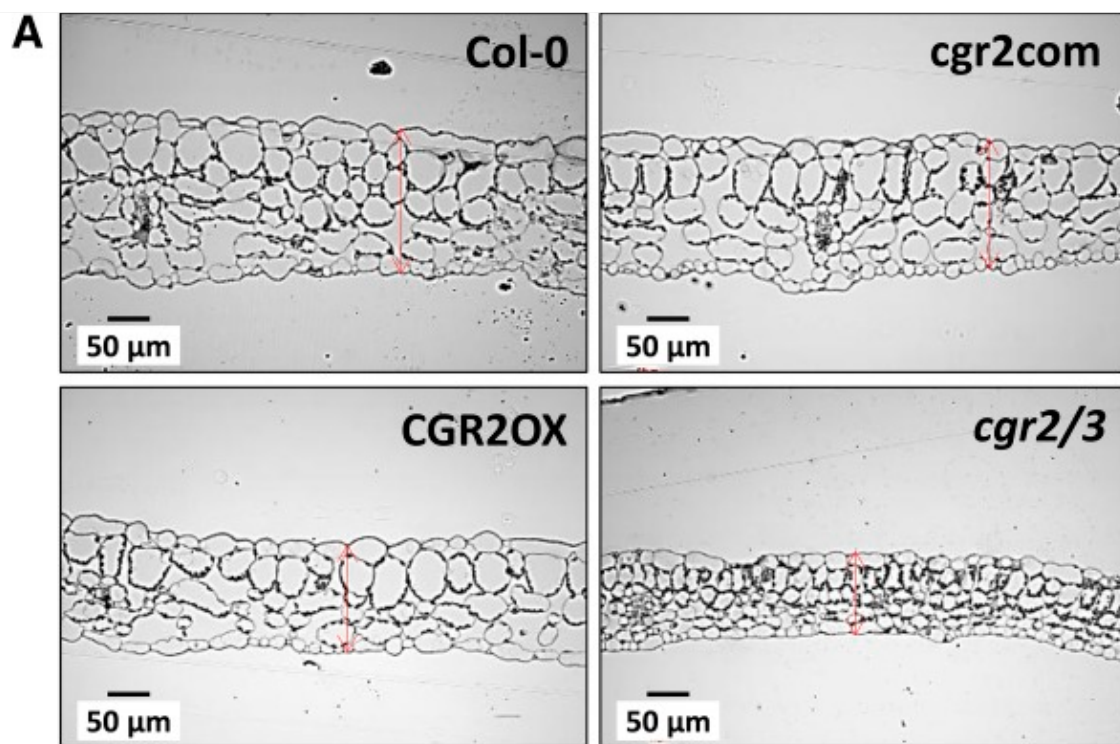
H1**H2****H3****H4**[Open in a new tab](#)

Projected and total leaf area over time in *Arabidopsis* with altered *CGR2* and *CGR3* expression. A, Projected leaf area and B, total leaf area at four different harvests (H) is presented for Col-0, *cgr2com*, *CGR2OX*, and *cgr2/3*. H1, H2, H3, and H4 correspond to 29, 49, 63, and 82 [DAS](#), respectively. For clarity, data for H1 is presented as insets in (A) and (B). Values represent the mean \pm SE and $n = 5$ plants per line. Statistical differences at $\alpha = 0.05$ are marked with lower-case letters.

Genetic Depletion of *CGR2* and *CGR3* Results in Thin Leaves with Small, Densely Packed Mesophyll Cells

Leaf area and thickness are generally negatively correlated ([Lambers et al., 2008](#); [Weraduwage et al., 2015](#)). To determine whether changes in leaf area in *CGR2OX* and *cgr2/3* were accompanied by changes in leaf thickness, we measured leaf thickness. Interestingly, leaves of *cgr2/3* were both thin and of small leaf area ([Fig. 2, A and B](#)); this trend was observed throughout the lifecycle (data not shown). During early vegetative growth [34 d after seeding ([DAS](#))], *CGR2OX* produced thinner leaves with a tendency toward more area than Col-0. Nonetheless, the *CGR2OX* leaves were thicker than those of *cgr2/3*.

Figure 2.

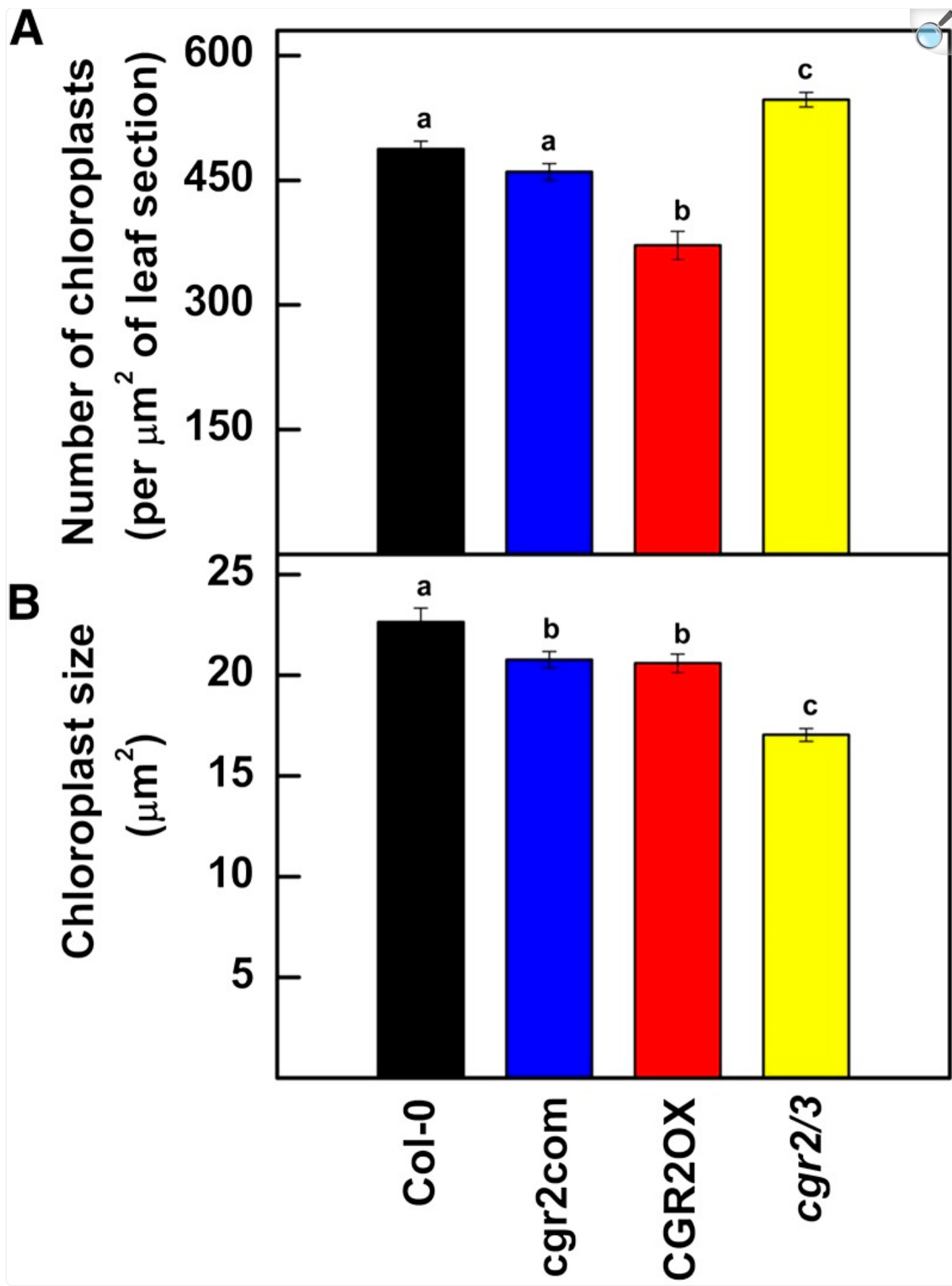


Leaf thickness and anatomy in *Arabidopsis* with altered *CGR2* and *CGR3* expression. A, Representative micrographs of leaf cross sections; B, leaf thickness; C, the relationship between the number of mesophyll cells and size of the intercellular air spaces in the leaf mesophyll; D, the surface area of mesophyll cells exposed to intercellular air spaces per unit leaf area (S_{mes}); and E, the surface area of chloroplasts exposed to intercellular air spaces per unit leaf area (S_c) are presented for Col-0, *cgr2com*, *CGR2OX*, and *cgr2/3*. In (A), leaf thickness is denoted by red double arrows. Data were obtained from 34-d old leaves. In (B), (D), and (E), values represent the mean \pm SE and $n = 4$ plants per line. In (C), $n = 4$ plants per line were used to obtain the mean values for the area of air spaces as a % of area of leaf cross section and the number of mesophyll cells per mm^2 of leaf cross section. Statistical differences at $\alpha = 0.05$ are marked with lower-case letters.

Next, we determined whether *CGR2*- and *CGR*-mediated pectin methylesterification was correlated with changes in mesophyll architecture. *CGR2OX* had larger palisade cells and 3 to 4 mesophyll cell layers compared to Col-0, which produced 4 to 5 layers of comparatively smaller palisade cells ([Fig. 2A](#)). However, the mesophyll cells of *cgr2/3* were significantly smaller and more numerous than in Col-0 ([Fig. 2A](#)), which led to a marked reduction in intercellular airspaces in the leaf mesophyll ([Fig. 2C](#)). Consequently, a significant negative correlation was observed between the number of cells and intercellular air spaces in the leaf mesophyll ([Fig. 2C](#)). Enhanced cell density and the reduction in intercellular air spaces in *cgr2/3* compared to the other *Arabidopsis* lines also led to a significant reduction in mesophyll cell surface area (S_{mes}) and chloroplast surface area (S_c) exposed to intercellular air spaces per unit leaf area ([Fig. 2, D and E](#)).

Interestingly also, the number of chloroplasts per unit area of a leaf cross section was lower in *CGR2OX* and greater in *cgr2/3* compared to Col-0 ([Fig. 3A](#)). However, the average size of chloroplasts was smaller in all transgenic lines compared to Col-0 ([Fig. 3B](#)). The data indicate that the reduction in S_c in *cgr2/3* was not a result of a reduction in chloroplast area per unit leaf area, but instead was linked to the significant reduction in intercellular air spaces in the leaf mesophyll. Therefore, our results show that variations in the levels of methylesterification of the cell wall significantly impact leaf thickness, cell density, and mesophyll architecture.

Figure 3.

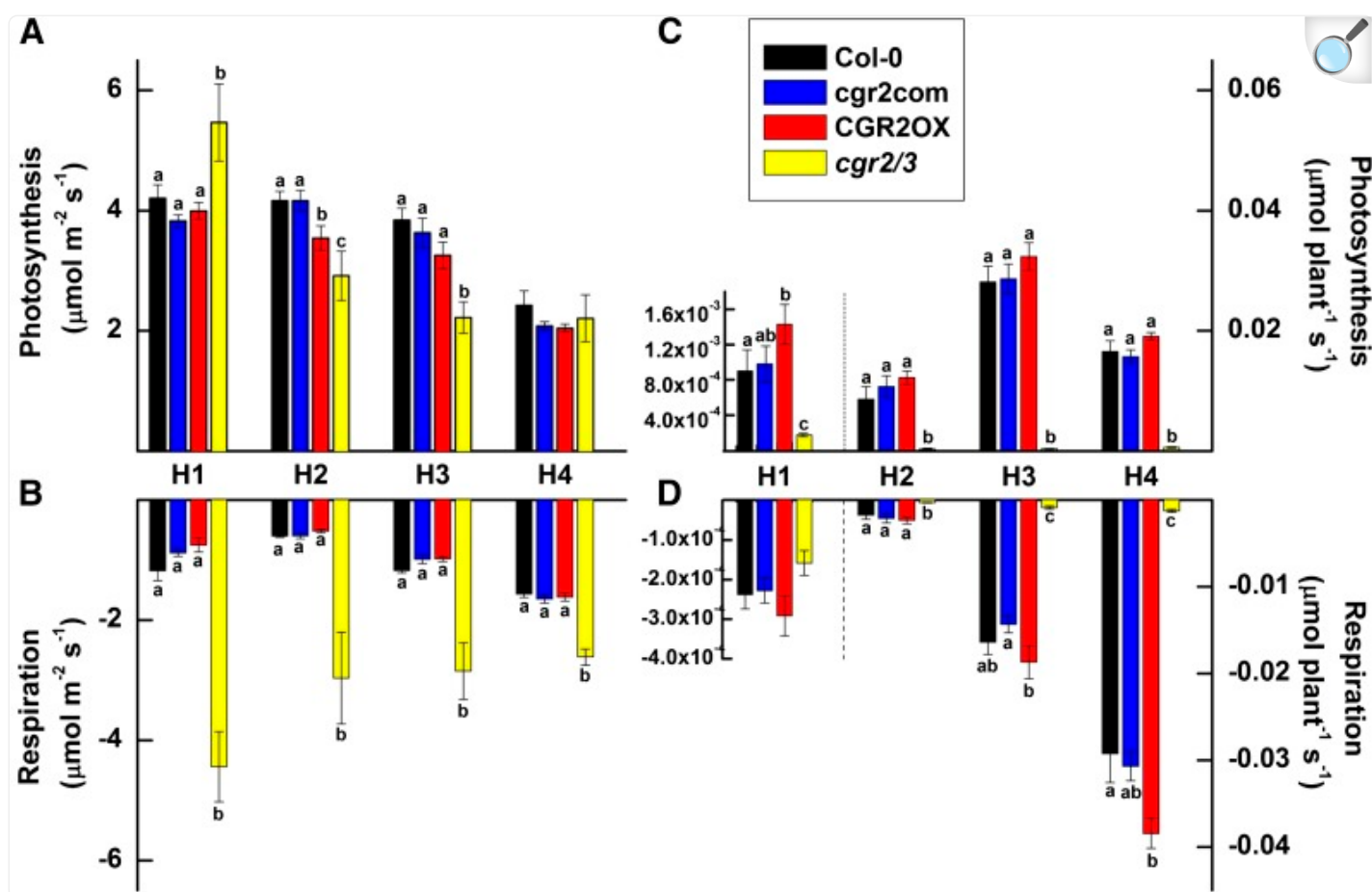


Abundance and size of chloroplasts in Arabidopsis with altered *CGR2* and *CGR3* expression. A, Number of chloroplasts per unit area of leaf cross section; B, Size of chloroplasts in 34-d-old leaves is shown for Col-0, *cgr2com*, *CGR2OX*, and *cgr2/3*. Values represent the mean \pm SE and $n = 12$. Statistical differences at $\alpha = 0.05$ are marked with lower-case letters.

Changes in Mesophyll Architecture due to Alterations in *CGR*-Expression Affected Area-Based Photosynthesis and Respiration

We next aimed to establish whether changes in mesophyll architecture as well as projected and total leaf areas affect net C assimilation in mutant lines with altered *CGR*-expression. To do this, we measured area- and plant-based photosynthesis and respiration. During early vegetative growth, at around 29 DAS, area-based photosynthesis in *cgr2/3* was significantly higher than the other lines ([Fig. 4A](#)). Afterward, *cgr2/3* showed lower area-based photosynthesis rates compared to Col-0 throughout the vegetative growth phase ([Fig. 4A](#)). Area-based photosynthesis in *CGR2OX* was lower than Col-0 around 49 [DAS](#), but remained higher compared to *cgr2/3*.

Figure 4.



[Open in a new tab](#)

Photosynthesis and respiration over time in Arabidopsis with altered *CGR2* and *CGR3* expression. A, Area-based photosynthesis, B, area-based nighttime respiration, C, photosynthesis on a whole plant basis, and D, night-time respiration on a whole plant basis at four different harvests (H) is shown for Col-0, *cgr2com*, *CGR2OX*, and *cgr2/3*. Photosynthesis (C gain) is shown as a positive number (A, C) while respiration (C loss) is shown as a negative number (B, D). H1, H2, H3, and H4 correspond to 29, 49, 63, and 82 [DAS](#), respectively. For clarity, the scale of the Y-axis for H1 in (C) and (D) is presented on the left-hand-side. Values represent the mean \pm SE and $n = 5$ plants per line. Statistical differences at $\alpha = 0.05$ are marked with lower-case letters.

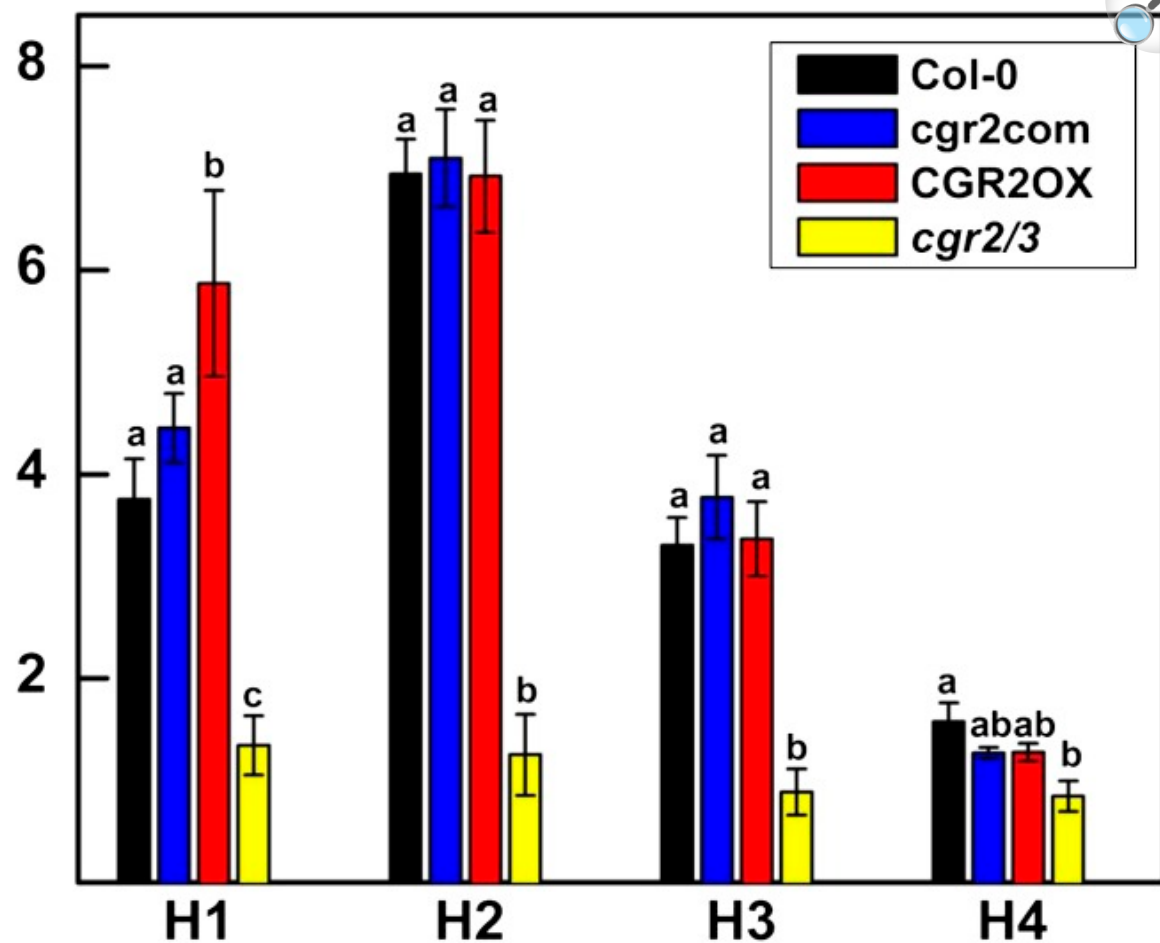
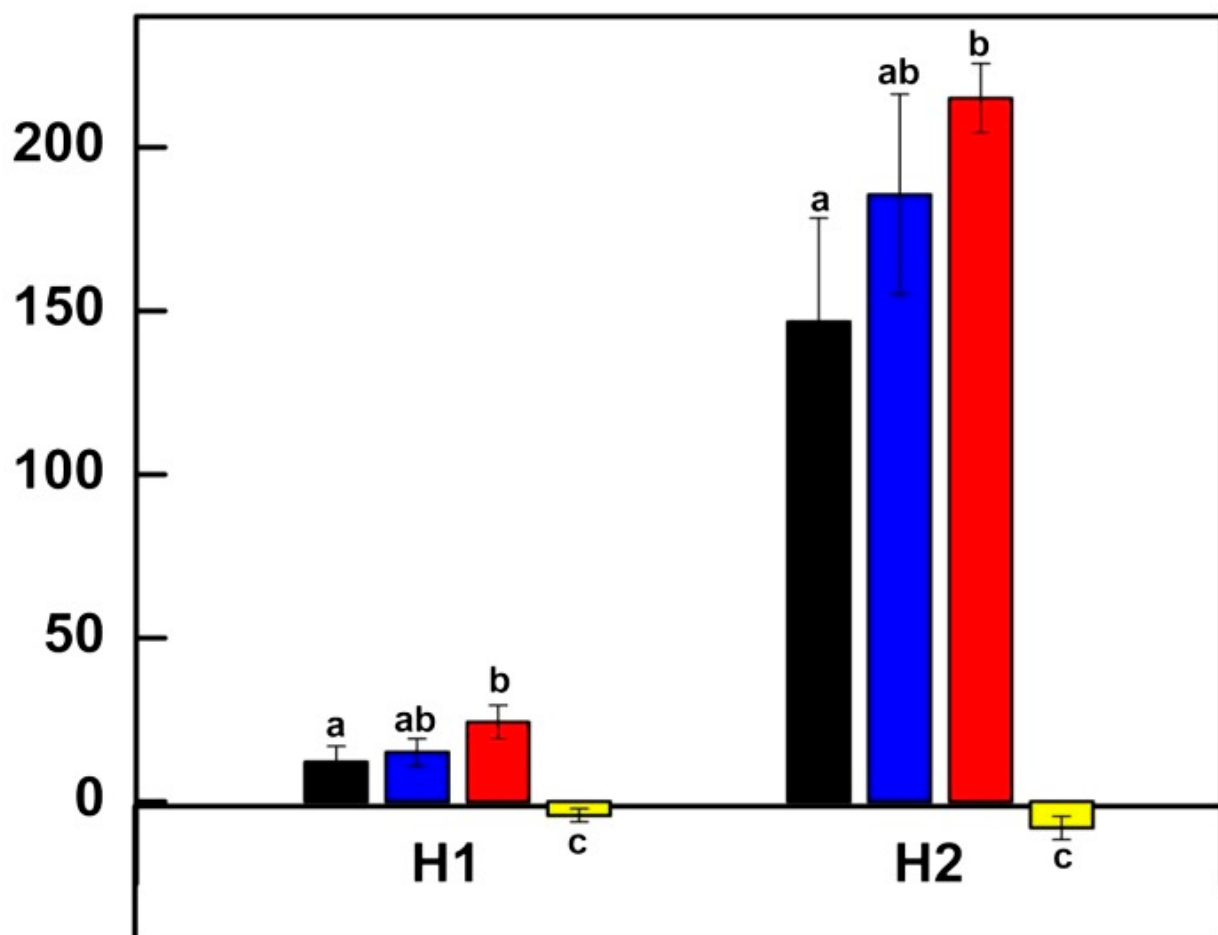
We also established that area-based respiration in *cgr2/3* was 2 to 5 times greater than Col-0 ([Fig. 4B](#)). Thus, photosynthesis/respiration ratio remained significantly smaller in *cgr2/3* throughout the lifecycle ([Fig. 5A](#)). Although not statistically significant at the 0.05 significance level, *CGR2OX* showed a trend toward lower area-based respiration

([Fig. 4B](#)) and therefore, its photosynthesis/respiration ratio appeared to be greater in young rosette leaves at 29 [DAS](#) ([Fig. 5A](#)). Increased area-based respiration in *cgr2/3* and lower area-based respiration in CGR2OX correlated well with the differences in the number of mesophyll cells in these lines ([Fig. 2C](#)). In general, plant-based photosynthesis in CGR2OX was similar to Col-0 with an upward trend, even though area-based photosynthesis was smaller ([Fig. 4, A and C](#)); this was mainly due to the larger projected leaf area in CGR2OX ([Fig. 1A](#)). However, owing to its smaller projected leaf area, plant-based photosynthesis in *cgr2/3* was much lower than Col-0 ([Fig. 4C](#)). Plant-based respiration was greater in CGR2OX, and smaller in *cgr2/3* than in Col-0 ([Fig. 4D](#)), which could be explained by differences in total leaf area ([Fig. 1B](#)).

Figure 5.

A

Photosynthesis:respiration ratio

**B**Daily C gain ($\mu\text{mol plant}^{-1} \text{ day}^{-1}$)

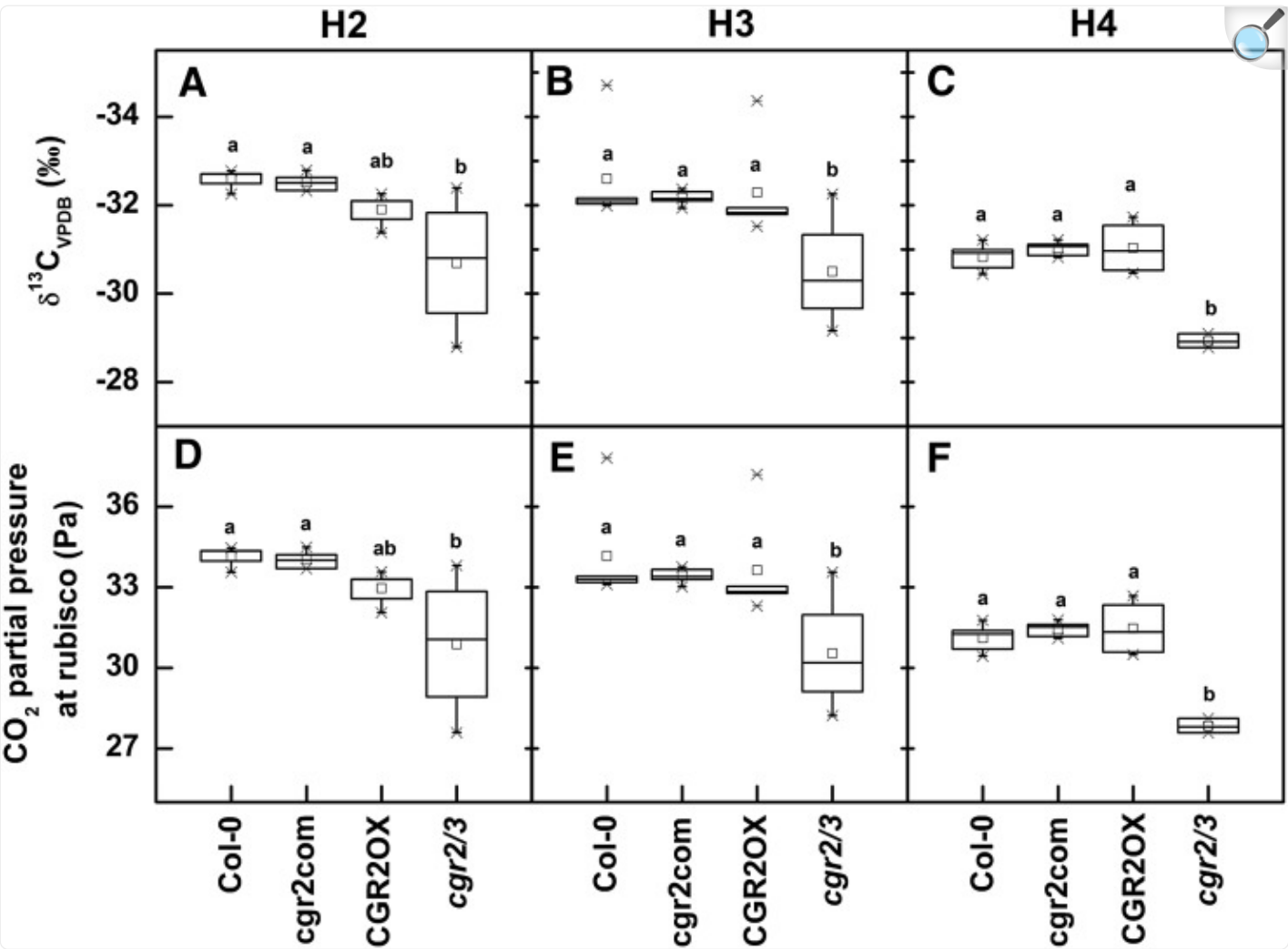
Daily C gain in Arabidopsis with altered *CGR2* and *CGR3* expression. A, Photosynthesis/respiration ratio at four different harvests (H); B, The daily C gain at two different harvests for Col-0, *cgr2com*, *CGR2OX*, and *cgr2/3* is given. H1, H2, H3, and H4 correspond to 29, 49, 63, and 82 [DAS](#), respectively. Values represent the mean \pm SE and $n = 5$ plants per line. Statistical differences at $\alpha = 0.05$ are marked with lower-case letters.

Daily C gain in rosettes was greater in *CGR2OX* compared to Col-0 when measured at 29 and 49 [DAS](#), while it was significantly smaller in *cgr2/3* ([Fig. 5B](#)). The upward trend in daily C gain observed in *CGR2OX* was a result of its higher plant-based photosynthetic rates due to greater projected leaf area ([Figs. 1A](#) and [4C](#)). The decrease in C gain in *cgr2/3* resulted from reduced plant-based photosynthesis due to the smaller projected leaf area and smaller photosynthesis/respiration ratio compared to *CGR2OX* ([Figs. 1A](#), [4C](#), and [5A](#)). Together these results support the hypothesis that by controlling leaf area and mesophyll architecture, pectin methylesterification is a critical factor for regulation of whole-plant rates of photosynthesis and respiration.

Suppression of Pectin Methylesterification Led to a Reduction in CO₂ Availability for Photosynthesis

The differences in chloroplast number and size could not account for the large differences observed in area-based photosynthesis between *cgr2/3* and the other three Arabidopsis lines ([Fig. 3, A and B](#)). Therefore, to investigate whether lower area-based photosynthesis rates in *cgr2/3* at harvests 2, 3, and 4 were a result of a reduction in CO₂ availability owing to altered mesophyll architecture, the degree of ¹³C discrimination was analyzed in leaf tissue of the four Arabidopsis lines. The ¹³C content of *cgr2/3* was greater, consistent with less discrimination against ¹³CO₂ during photosynthesis compared to the other lines ([Fig. 6, A–C](#)). The average CO₂ partial pressure at Rubisco calculated using the $\delta^{13}\text{C}_{\text{VPDB}}$ (Vienna-Pee-Dee Belemnite, [VPDB](#)) values showed CO₂ availability to be significantly lower in *cgr2/3* ([Fig. 6, D–F](#)). These data are in agreement with the hypothesis that there is a greater resistance to CO₂ diffusion into chloroplasts of *cgr2/3*, owing to lower surface areas of mesophyll cells and chloroplasts facing intercellular air spaces per unit leaf area as a result of enhanced cell density and reduced intercellular air spaces ([Fig. 2, C–E](#)). Therefore, reduction in *CGR2* and *CGR3* availability appears to have a strong negative impact on area-based photosynthesis owing to reduction in CO₂ availability to chloroplasts, most likely as a result of altered mesophyll architecture.

Figure 6.



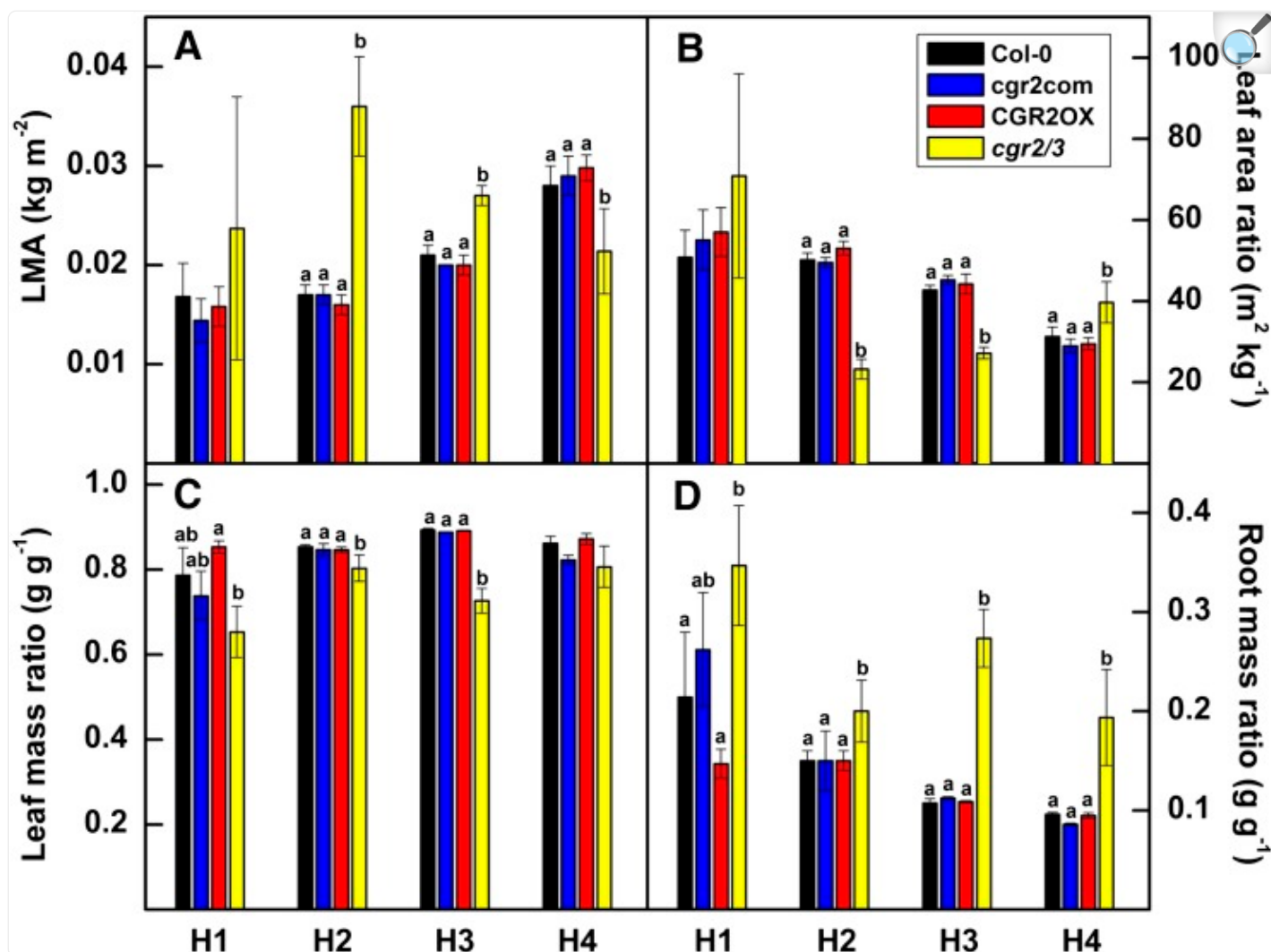
[Open in a new tab](#)

Degree of resistance to CO₂ diffusion through the leaf mesophyll over time in Arabidopsis with altered *CGR2* and *CGR3* expression. A, B, C, The $\delta^{13}\text{C}_{\text{VPDB}}$ value calculated as the ratio of ^{13}C to ^{12}C isotopes in leaf tissue relative to a [VPDB](#) value; D, E, F, CO₂ partial pressure at Rubisco at three different harvests (H) is shown for Col-0, cgr2com, CGR2OX, and cgr2/3. H2, H3, and H4 correspond to 49, 63, and 82 [DAS](#), respectively. Values represent the mean \pm SE and $n = 5$ plants per line. Statistical differences at $\alpha = 0.05$ are marked with lower-case letters.

A Decrease in Pectin Methylesterification Increased [LMA](#), and Reduced Plant Growth and Relative Growth Rates

We next analyzed the effects of altered expression of *CGR2* and *CGR3* on plant growth by measuring leaf growth parameters, plant biomass, and relative growth rates. We found that [LMA](#) was higher in *cgr2/3* during the early to late vegetative phases, around 29 to 63 [DAS](#) ([Fig. 7A](#)). In addition, [LMA](#) in *CGR2OX* remained significantly lower than in *cgr2/3*. Leaf area per unit plant mass (leaf area ratio) and leaf mass ratio (mass of leaf per unit plant mass) were significantly smaller in *cgr2/3* than other lines ([Fig. 7, B and C](#)). In contrast, root mass ratio (mass of root per unit plant mass) was larger in *cgr2/3* than other lines ([Fig. 7D](#)).

Figure 7.



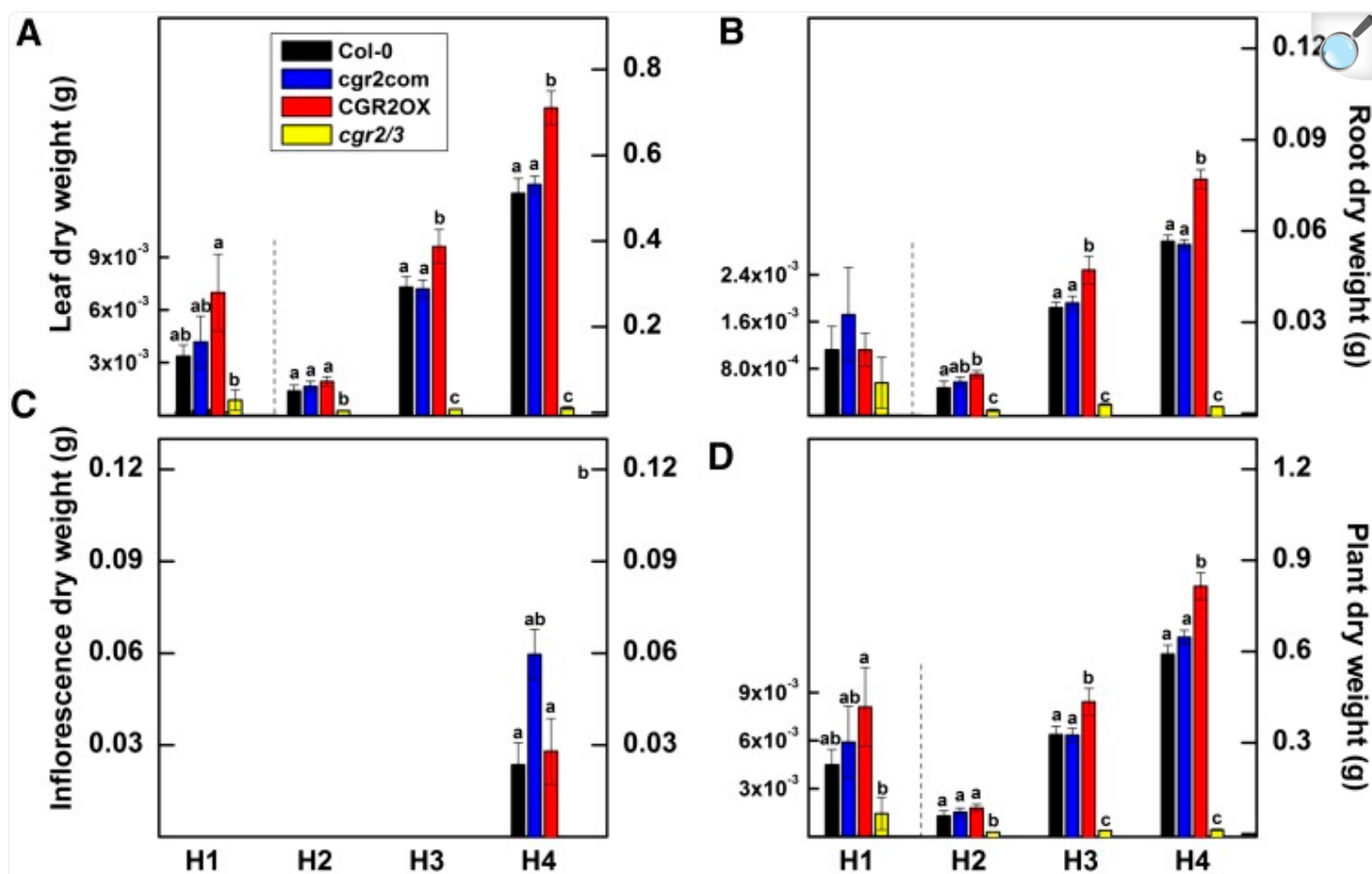
[Open in a new tab](#)

Variations in leaf growth parameters over time in Arabidopsis with altered *CGR2* and *CGR3* expression. A, [LMA](#), B, leaf area ratio, C, leaf mass ratio, and D, root mass ratio at four different harvests (H) for Col-0, *cgr2com*, *CGR2OX*, and *cgr2/3* is presented. H1, H2, H3, and H4 correspond to 29, 49, 63, and 82 [DAS](#), respectively. Values represent the mean and $n = 5$ plants per line. Statistical differences at $\alpha = 0.05$ are marked with lower-case letters.

Interestingly, *CGR2OX* maintained the greatest leaf, root, and plant biomass throughout the lifecycle ([Fig. 8, A–D](#)). In contrast, *cgr2/3* plants exhibited a significant reduction in leaf, root, and plant dry weight throughout the lifecycle. Collectively, these data reveal that alterations in *CGR2* and *CGR3* expression can have a significant effect not only on

leaf growth, but also on overall plant growth. Therefore, while an increase in pectin methylesterification enhances plant biomass, a decrease in pectin methylesterification reduces it. Modeled relative growth rates revealed that both area-based ([Fig. 9A](#)) and mass-based ([Fig. 9B](#)) relative growth rates were higher in *CGR2OX* and smaller in *cgr2/3* than Col-0 during most part of the lifecycle. In summary, alterations in *CGR2* and *CGR3* have a significant impact on important leaf growth parameters such as [LMA](#), and biomass partitioning to leaf growth, and also affect plant growth in terms of biomass accumulation and relative growth rates. [LMA](#) showed a negative correlation with plant growth and relative growth rates.

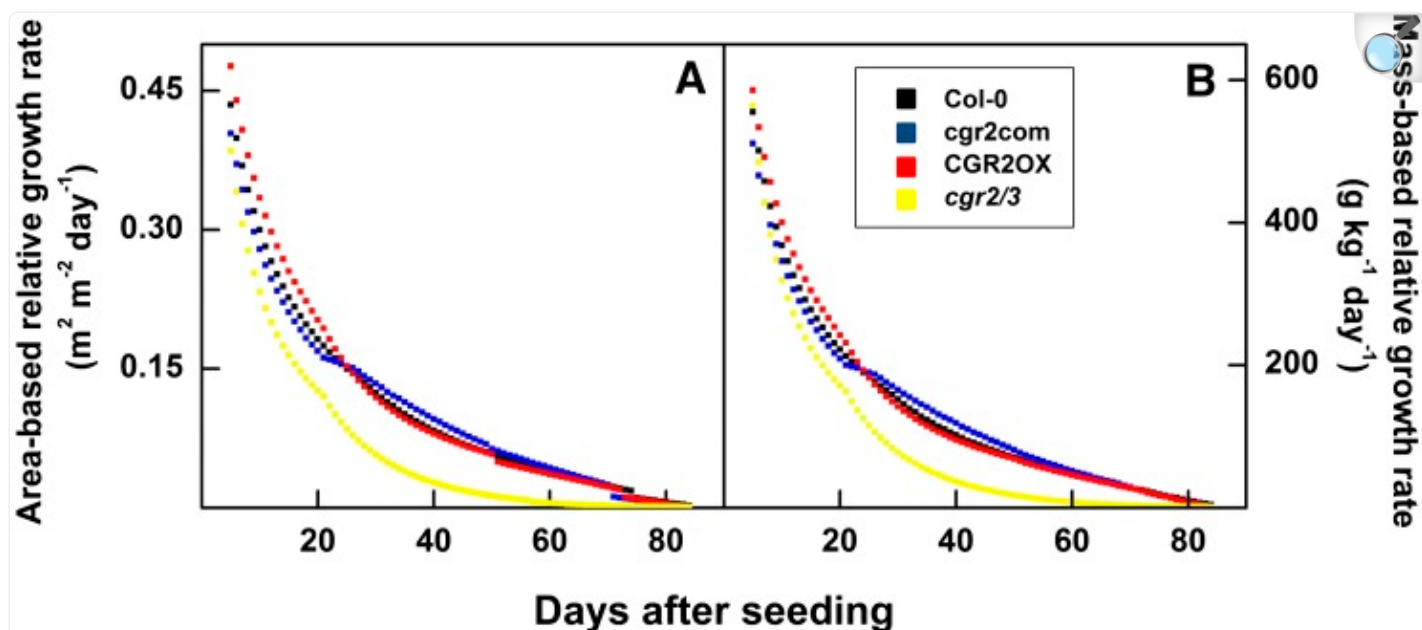
Figure 8.



[Open in a new tab](#)

Variations in dry weight over time in Arabidopsis with altered *CGR2* and *CGR3* expression. A, Leaf, B, root, C, inflorescence, and D, whole plant dry weight at four different harvests (H) for Col-0, *cgr2com*, CGR2OX, and *cgr2/3* is given. H1, H2, H3, and H4 correspond to 29, 49, 63, and 82 DAS, respectively. For clarity, the scale of the Y-axis for H1 in (A), (B) and (C) is presented on the left-hand-side. Values represent the mean \pm SE and $n = 5$ plants per line. Statistical differences at $\alpha = 0.05$ are marked with lower-case letters.

Figure 9.



[Open in a new tab](#)

Modeled relative growth rates over time in Arabidopsis with altered *CGR2* and *CGR3* expression. A, Area-based relative growth rates and B, mass-based relative growth rates simulated from days 5 to 84 using the Arabidopsis leaf area growth model fitted with data obtained from Col-0, *cgr2com*, *CGR2OX*, and *cgr2/3* are presented.

Enhanced Pectin Methylesterification and C Partitioning to Leaf Area Growth

The Arabidopsis leaf area growth model parameterized with measurements obtained from the four Arabidopsis lines was used to estimate how much C was partitioned to new leaf area growth and *LMA*, as a proportion of net assimilated C that is available for growth. These values, referred to as partitioning coefficients (*Table I*), would allow determination of whether changes in *CGR2* and *CGR3* availability could affect C partitioning to growth or respiratory processes. The proportions of C partitioned to leaf growth in total (C partitioned to area + *LMA*), and to root growth found by $^{14}\text{CO}_2$ feeding experiments at 29 *DAS*, were used as an initial estimate when setting the partitioning coefficients to leaf growth for the early vegetative growth phase (*Supplemental Fig. S4* ; *Table I*). Partitioning coefficients obtained from growth modeling for *CGR2OX* revealed that, compared to the other lines, the *CGR2* over-expression line partitioned more of the C available for leaf growth toward leaf area growth and less toward *LMA*, especially during the early vegetative phase (*Table I*). In contrast, we found that in *cgr2/3* a significantly greater proportion of C was allocated to *LMA* rather

than to leaf area growth ([Table I](#)). The differences in C partitioning to leaf area growth and [LMA](#) between Col-0 and CGR2OX and *cgr2/3* were most prominent during early vegetative phases of growth.

Table I. Comparison of modeled partitioning coefficients during different growth phases for Arabidopsis lines with altered pectin methyltransferase expression.

Arabidopsis line	Organ/process to which C is partitioned	Partitioning coefficients		
		Early vegetative growth phase	Late vegetative growth phase	Reproductive growth phase
Col-0	Inflorescence growth	0.00	0.02	0.30
	Root growth	0.06	0.13	0.12
	LMA	0.17	0.10	0.10
	Leaf area growth	0.77	0.75	0.48
cgr2com	Inflorescence growth	0.00	0.03	0.40
	Root growth	0.03	0.12	0.12
	LMA	0.19	0.10	0.10
	Leaf area growth	0.78	0.75	0.38
CGR2OX	Inflorescence growth	0.00	0.03	0.30
	Root growth	0.04	0.15	0.15
	LMA	0.16	0.11	0.10
	Leaf area growth	0.80	0.71	0.45
cgr2/3	Inflorescence growth	0.00	0.00	0.10
	Root growth	0.10	0.25	0.25
	LMA	0.24	0.18	0.10
	Leaf area growth	0.66	0.57	0.55

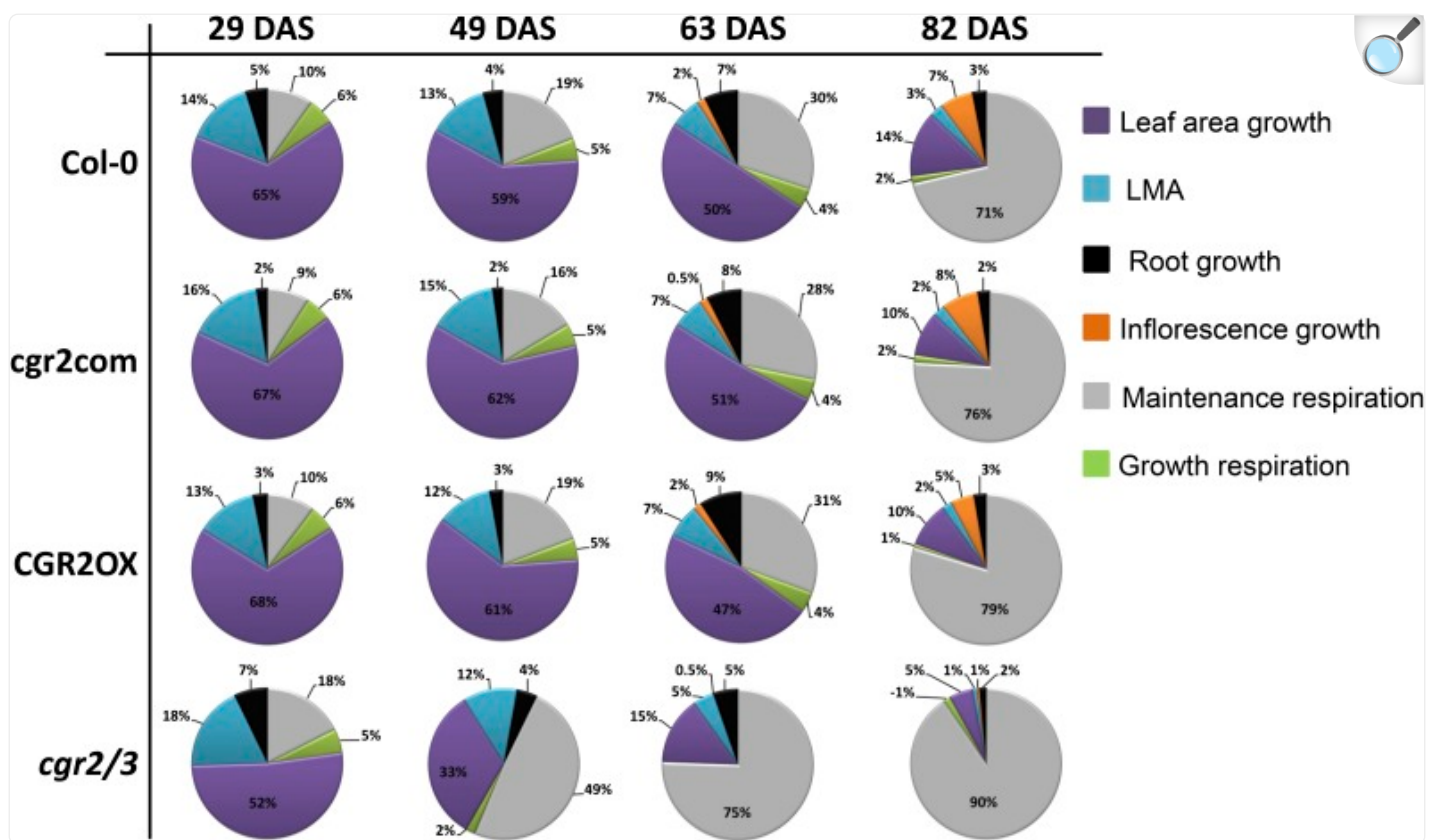
[Open in a new tab](#)

Partitioning coefficients for partitioning of net assimilated C to inflorescence and root growth, [LMA](#), and leaf area growth during the early and late vegetative phases and the reproductive phase for Col-0, cgr2com, CGR2OX, and cgr2/3 were obtained from the Arabidopsis leaf area growth model. The durations of the early and late vegetative phases and the reproductive phase for each line is as follows: for Col-0, 5–51 [DAS](#), 52–74 [DAS](#), and 75–90 [DAS](#); for cgr2com, 5–48 [DAS](#), 49–70 [DAS](#), and 71–90 [DAS](#); for CGR2OX, 5–49 [DAS](#), 50–

72 [DAS](#), and 73–90 [DAS](#); and for *cgr2/3*, assuming flower initiation started at 82 [DAS](#), 5–55 [DAS](#), 56–81 [DAS](#), and 82–90 [DAS](#).

The patterns of C partitioning in transgenic lines seen in [Table I](#) were further investigated by determining the amounts of C being partitioned to specific growth processes as well as respiratory processes as a proportion of the total available C in the plant ([Fig. 10](#)). CGR2OX still partitioned a greater proportion of total available C to leaf area growth and a lesser proportion to [LMA](#) compared to the other lines; *cgr2/3* showed an opposite trend to that seen in CGR2OX ([Fig. 10](#)). The maintenance respiratory cost increased as the plant aged. Toward the end of its lifecycle (82 [DAS](#)), close to 75% of assimilated C was consumed in maintenance respiration ([Fig. 10](#)). While the maintenance costs in CGR2OX were somewhat larger than Col-0 toward the end of the lifecycle, a significant enhancement in the proportion of C spent in maintenance respiration could be seen in *cgr2/3* throughout the lifecycle ([Fig. 10](#)). Collectively, these data provide evidence to support that alteration in *CGR2* and *CGR3* expression has a significant impact on determining the proportions of C partitioned to new leaf area growth versus [LMA](#), and to maintenance respiration in plants.

Figure 10.



[Open in a new tab](#)

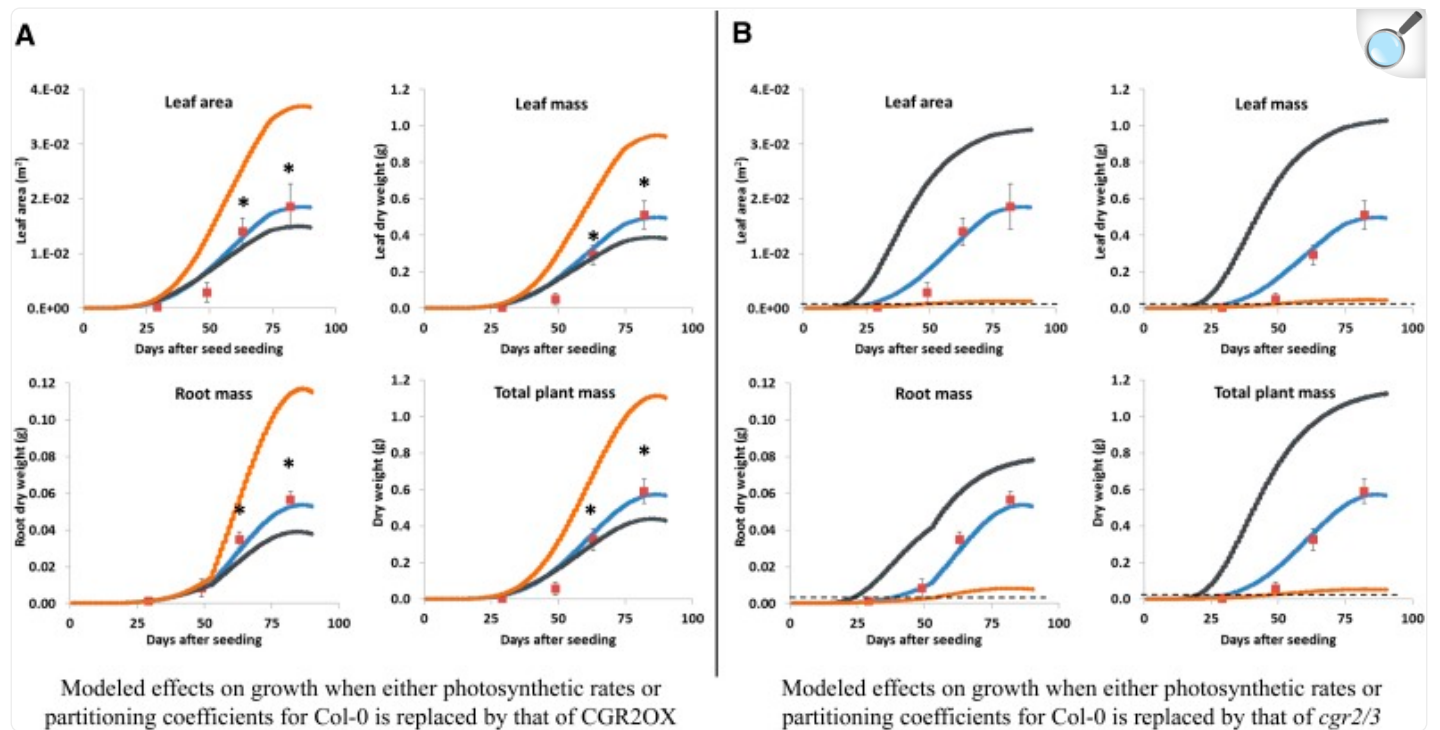
Modeled C partitioning to growth and respiration in Arabidopsis with altered *CGR2* and *CGR3* expression. Carbon partitioned to support growth in terms of leaf area and [LMA](#), and inflorescence growth, root growth, and maintenance and growth respiration is presented as percentages of the daily available C at 29, 49, 63, and 82 [DAS](#). Data were derived from the Arabidopsis leaf area growth model fitted with data obtained from Col-0, *cgr2com*, *CGR2OX*, and *cgr2/3*.

Growth in *CGR2OX* and *cgr2/3* was Affected More by Alterations in C Partitioning than by Changes in Area-Based Photosynthesis

To determine whether the alterations in growth observed in *CGR2OX* and *cgr2/3* were a result of alterations in area-based photosynthesis ([Fig. 4A](#)) or partitioning coefficients to leaf area growth and [LMA](#) growth ([Table I](#)), the values for these parameters in the growth model for Col-0 were substituted separately by corresponding values from the two transgenic lines. Interestingly, by keeping the partitioning coefficients the same, substitution of area-based

photosynthesis rates for 1 to 90 d with those of CGR2OX resulted in a small reduction in modeled growth in Col-0 whereas *cgr2/3* caused a large increase in growth (gray lines in [Fig. 11](#)).

Figure 11.



[Open in a new tab](#)

Comparison of the effects of altered area-based photosynthesis and C partitioning coefficients on plant growth in Arabidopsis with altered *CGR2* and *CGR3* expression. Modeled effects on leaf area and leaf, root, and plant dry weights when either photosynthetic rates or partitioning coefficients spanning the entire growth cycle for Col-0 are replaced by those of (A) CGR2OX and (B) *cgr2/3* are presented. In (A) and (B), blue lines represent modeled growth for Col-0, and red squares represent measured data points (mean ± SD) for Col-0 at 29, 49, 63, and 82 [DAS](#). Gray lines represent modeled data for Col-0 when its area-based photosynthesis rates are replaced by that of either CGR2OX (A) or *cgr2/3* (B). Orange lines represent modeled data for Col-0 when its partitioning coefficients ([Table I](#)) are replaced by that of either CGR2OX (A) or *cgr2/3* (B) without making any changes to area-based photosynthesis rates of Col-0. In (A), asterisks represent measured data for CGR2OX at 63 and 82 DAS. In (B), the dotted line indicates the upper limit of measured data for *cgr2/3*.

However, by keeping area-based photosynthesis the same, substituting the partitioning coefficients of Col-0 with that of

CGR2OX had a strikingly large positive effect on modeled growth; *cgr2/3* partitioning coefficients had a significantly large negative effect on growth that mirrored the observed differences in growth in the *CGR2* over-expression line and the *CGR2* and *CGR3* double mutant line (orange lines in [Fig. 11](#)). These observed changes in growth could be achieved by substituting the partitioning coefficients of only the early vegetative growth phase (data not shown). The data show that the observed changes plant growth in CGR2OX and *cgr2/3* were not a result of differences in photosynthetic rates, but a result of differences in C partitioning to growth in terms of leaf area and [LMA](#), especially during early vegetative growth. Thus, our data support the hypothesis that the magnitude of plant growth is determined by how photosynthetic C is partitioned to new leaf area growth and [LMA](#).

DISCUSSION

In this study, we investigated how modification of cell wall plasticity via the genetic manipulation of pectin methyltransferases, *CGR2* and *CGR3*, affects C assimilation, leaf respiration, and overall plant growth through effects on leaf area growth and mesophyll structure. We also wanted to further understand the relationship between photosynthesis and plant growth by determining whether the changes in overall plant growth in Arabidopsis with altered cellular availability of *CGR2* and *CGR3* were a result of changes in growth in terms of leaf area and [LMA](#) or due to changes in area-based photosynthesis. We found that over-expression of *CGR2* had a significant positive effect on leaf area and plant growth. On the other hand, suppression of *CGR2* and *CGR3* expression caused a marked increase in [LMA](#) and a reduction in leaf area and plant growth. Altered expression of *CGR2* and *CGR3* also had a significant impact on photosynthesis and respiration through altered mesophyll architecture. The differences in plant growth in Arabidopsis with altered *CGR2* and *CGR3* levels were linked to changes in C partitioning to leaf area growth and [LMA](#) rather than altered area-based photosynthesis rates. These findings establish that *CGR2*- and *CGR3*-mediated pectin methylesterification affects mesophyll architecture, C accumulation, C partitioning, leaf and plant growth, and the relationship between photosynthesis and plant growth.

CGR2 and *CGR3* Directly Affect Leaf Mass per Unit Area by Altering Both Leaf Thickness and the Mass of Leaf per Unit Volume of Leaf Tissue

Often, thicker leaves are associated with larger [LMA](#) due to an increase in the number of cell layers, which can increase leaf mass per unit leaf area ([Lambers et al., 2008](#); [Poorter et al., 2009](#); [Villar et al., 2013](#); [Weraduwaage et al., 2015](#)). However, a negative correlation exists between leaf mass density or [LMD](#) (mass of leaf per unit volume of leaf tissue) and leaf thickness, and both parameters can affect [LMA](#) as follows: $\text{LMD (kg m}^{-3}\text{)} = \text{leaf mass}/(\text{leaf area} \times \text{leaf thickness})$ and $\text{LMA (kg m}^{-2}\text{)} = \text{LMD} \times \text{leaf thickness}$ ([Witkowski and Lamont, 1991](#); [Lambers et al., 2008](#); [Poorter et al., 2009](#); [Villar et al., 2013](#)). Therefore, leaf thickening or an increase in [LMA](#) can occur due to an increase in leaf thickness or [LMD](#). While thicker leaves have been shown to be associated with larger mesophyll cells (elongated, especially in the depth direction) and larger air spaces, [LMD](#) has been associated with smaller proportions of

intercellular air spaces and smaller cells ([Tsuge et al., 1996](#); [Poorter et al., 2009](#); [Villar et al., 2013](#)). In addition to being affected by anatomical changes, [LMA](#) and [LMD](#) can also be determined by variations in cellular and chemical composition ([Cunningham et al., 1999](#); [Lambers et al., 2008](#)). For example, plants with slow growth rates possess a larger number of smaller cells with thicker cell walls, and a greater proportion of lignin and other cell wall polysaccharides per unit leaf area that can increase [LMD](#) and [LMA](#) ([Cunningham et al., 1999](#); [Lambers et al., 2008](#)). A key aspect of cellular mass is represented by organelles, and plants with higher growth rates may possess large cells with a lower number of chloroplasts, which results in lower [LMA](#) ([Lambers et al., 2008](#)).

Interestingly, while both CGR2OX and *cgr2/3* had thinner leaves compared to Col-0, *cgr2/3* showed a significant increase in [LMA](#). Such increase in *cgr2/3* can be attributed to increased [LMD](#) as a result of enhanced cell density and reduction of intercellular air spaces in the leaf mesophyll. Smaller cells can lead to concentration of cellular metabolites, which can also lead to increased [LMD](#). In addition, *cgr2/3* also possessed a larger number of chloroplasts per unit leaf area. The proportions of cell wall components per unit leaf area are also likely greater in *cgr2/3* compared to the other backgrounds. Therefore, collectively the data clearly show that although *cgr2/3* had thinner leaves, enhanced [LMD](#) led to greater leaf mass per unit area (or lower [SLA](#)) in *cgr2/3*. Conversely, [LMA](#) in CGR2OX was significantly smaller than *cgr2/3*. Leaves of CGR2OX were also thicker than *cgr2/3* and contained larger intercellular airspaces, and larger cells with a lower number of chloroplasts. Therefore, our results support that variation in [LMA](#) between CGR2OX and *cgr2/3* resulted from the combination of increased leaf thickness and reduced leaf mass density.

The significant alterations in mesophyll architecture observed during this study are linked to changes in *CGR2* and *CGR3* expression. Based on the model that reduced methylation of pectin may enhance Ca^{2+} -mediated cross linking of GalUA in cell walls, thereby preventing normal cell expansion in *cgr2/3* ([Burton et al., 2000](#); [Wolf et al., 2009](#); [Kim et al., 2015](#)), we propose that the larger number of smaller mesophyll cells observed in *cgr2/3* during this study is likely linked to the hardening of the cell wall and consequent restriction of cell wall expansion. This in turn is likely to cause an increase of the cell number per unit leaf area in *cgr2/3* compared to Col-0. In addition, cross linking between GalUA and Ca^{2+} in cell wall pectin is required for cellular adhesion ([Caffall and Mohnen, 2009](#)). Also a reduction in GalUA- Ca^{2+} complex formation in *Solanum lycopersicum* resulted in large air spaces in the fruit pericarp caused by dramatic reductions in the middle-lamellae-mediated cell-to-cell adhesion ([Caffall and Mohnen, 2009](#)). The observed decrease in air spaces in *cgr2/3* and the dense distribution of the cells (hence thinner leaves) are likely due to enhanced cell-to-cell adhesion because of the lower degree of methylesterified pectin in *cgr2/3* compared to Col-0. In contrast, enhanced methylation of pectin promotes cell expansion ([Kim et al., 2015](#)); this resulted in the observed presence of wider palisade cells and a lower number of cell layers (hence thinner leaves) in CGR2OX than Col-0. The number of cells and area of airspaces in CGR2OX differed only marginally from Col-0. However, CGR2OX did have a smaller number of smaller chloroplasts compared to Col-0, which may be an indication of lower [LMA](#). Whether over-expression of *CGR2* has a dosage effect, and over-expression of both *CGR2* and *CGR3* would result in larger and thicker leaves with lower cell density remains to be investigated.

Thinner leaves usually correlate with larger [SLA](#) or smaller [LMA](#) ([Lambers et al., 2008](#); [Weraduwage et al., 2015](#)). However, based on the negative correlation between [LMD](#) and leaf thickness, it is likely that [LMD](#) would start to increase should leaf thickness decrease below a certain optimum, thereby resulting in an increase in [LMA](#). This was demonstrated in *cgr2/3*, where suppression of *CGR2* and *CGR3* resulted in leaves that were too thin, leading to higher cell density and [LMA](#). This can have significant negative effects on leaf gas exchange properties and daily C gain, as discussed below. The above phenotype was rescued by complementing with *CGR2*, as seen in *cgr2com* or by over-expressing *CGR2* as in *CGR2OX*. Thus, the degree of *CGR2*- and *CGR3*-mediated pectin methyl esterification can directly affect [LMA](#) by altering both leaf thickness and leaf mass density.

***CGR2* and *CGR3* Affect Area-Based Respiration and Daily C Gain by Altering [LMD](#) and [LMA](#)**

In general, leaves growing under high light develop thicker leaves with multiple cell layers and higher [LMA](#) (lower [SLA](#)), and incurs higher area-based respiration rates corresponding to their greater mass per unit leaf area ([Mitchell et al., 1999](#); [Lambers et al., 2008](#)). In contrast, plants grown under low light have lower [LMA](#) (higher [SLA](#)), which optimizes light capture and lowers area-based respiration rates ([Lambers et al., 2008](#)). This assists in maximizing daily C gain and compensates for lower area-based photosynthesis rates when growing under low light conditions ([Lambers et al., 2008](#)). Although *cgr2/3* produced thinner leaves, the marked enhancement in area-based respiration positively correlated with enhanced leaf cell density and higher [LMA](#). Higher area-based respiratory rates led to smaller photosynthesis/respiration ratio, and when coupled with smaller projected leaf area, they had a significant negative impact on daily carbon gain. Thus, pectin methylesterification affects area-based respiration rates through alterations in leaf cell density, [LMD](#), and [LMA](#) and consequently affect photosynthetic efficiency in plants.

***CGR2* and *CGR3* Directly Affect Area-Based Photosynthesis by Altering Mesophyll Architecture**

Diffusion of CO₂ into chloroplasts occurs along the path that poses the least resistance through the cell wall, plasma membrane, chloroplast envelope, and into the chloroplast stroma ([Terashima et al., 2006](#)). Therefore, S_c represents the active area through which CO₂ diffuses in to the chloroplast stroma ([Terashima et al., 2006](#)). A decrease in S_c leads to a reduction in CO₂ concentration at Rubisco and therefore to a reduction in the carboxylation/oxygenation ratio ([Terashima et al., 2006](#)). Parameters that affect CO₂ diffusion into the chloroplast stroma are thickness of the mesophyll cell wall, internal conductance to CO₂ diffusion, and stomatal conductance ([Terashima et al., 2006](#)). S_c has been shown to be positively correlated with internal conductance, while the latter is negatively correlated with cell wall thickness ([Terashima et al., 2006](#)).

In contrast to our original hypothesis, area-based photosynthesis rates were significantly lower in *cgr2/3* for most of the

lifecycle, even though this mutant possessed smaller projected leaf area and denser leaves. This study revealed that this reduction in area-based photosynthesis in *cgr2/3* was not a result of differences in chloroplast number and size, but, mainly a result of a reduction in CO₂ partial pressure at Rubisco due to restrictions imposed on CO₂ diffusion by increased cell density and reduced airspaces in the leaf mesophyll that lowered S_c . Preliminary investigations revealed that stomatal conductance is not negatively impacted in the mutant lines examined during this study (data not shown). Therefore, the observed reduction in area-based photosynthetic rates is most probably due to a cumulative effect of lower S_c , higher internal resistance and greater cell wall thickness per unit area. The greater area-based photosynthesis rates in *cgr2/3* observed during early stages of vegetative development may have been a result of leaves and cell walls being comparatively thinner in young plants. S_c values and CO₂ partial pressure at Rubisco in *cgr2/3* were restored to the levels of Col-0 in *cgr2com* owing to alterations brought about by *CGR2* expression in its leaf anatomy: thicker leaves with less dense mesophyll and more intercellular air spaces. S_c and CO₂ partial pressure in *CGR2OX* were similar to that of Col-0. The lower area-based photosynthesis in *CGR2OX* may have resulted from thinner but larger leaves, which may have then resulted in less photosynthetic machinery per unit leaf area. Correspondingly, chloroplast number and size were lower in *CGR2OX*. These data emphasize the importance of pectin methylesterification in fine-tuning cell expansion and size and cell-to-cell adhesion qualities in building a leaf mesophyll optimized for CO₂ exchange. While thin leaves are associated with lower [LMA](#) (or enhanced [SLA](#)), it is important to maintain an optimum thickness to maintain sufficient intercellular air spaces, which would maintain high internal conductance, S_{mes} , and S_c , and therefore higher carboxylation rates.

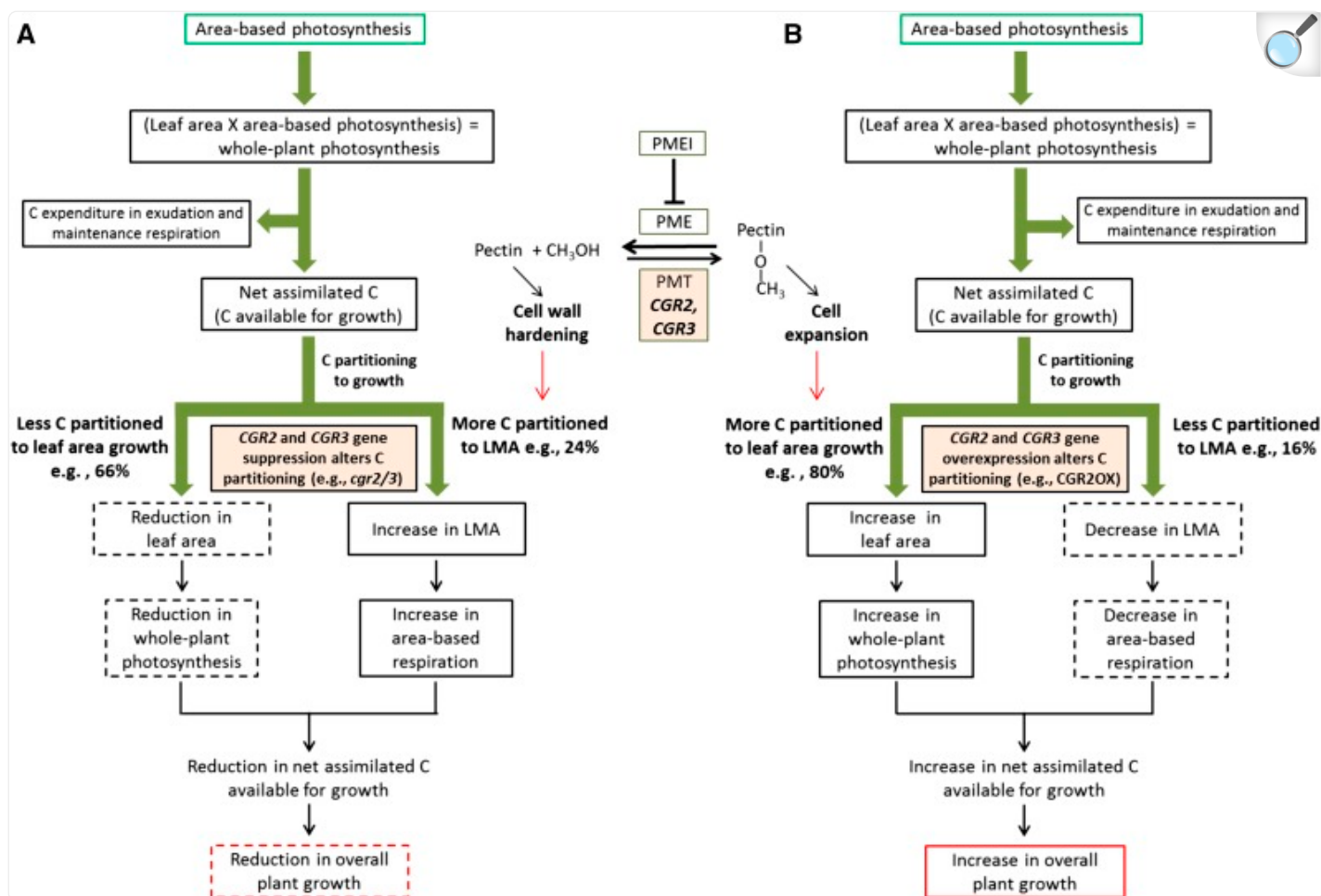
Pectin Methylesterification Mediates the Relationship between Photosynthesis and Plant Growth through Alterations in C Partitioning to Leaf Area Growth and Thickening

As hypothesized, suppression of *CGR2*- and *CGR3*-mediated pectin methylesterification had a profound negative effect on leaf area growth while over-expression of *CGR2* significantly enhanced leaf area growth. Suppression of *CGR2* and *CGR3* also led to a reduction in plant dry weight. Over-expression of *CGR2* enhanced plant dry weight. Growth modeling revealed that the observed variations in growth were not caused by changes in area-based photosynthesis. In fact, high rates of area-based photosynthesis measured in *cgr2/3* during early growth were found to be sufficient to drive growth higher than that seen in Col-0. Thus, growth had the opposite trend (*CGROX* > Col-0 > *cgr2/3*) compared with area-based photosynthetic rate (*cgr2/3* > Col-0 > *CGROX*). To account for enhanced overall plant growth, the amount of net assimilated C available for growth has to increase, which will depend on the total amount of C assimilated and the amount of C respired to support maintenance processes ([Weraduwage et al., 2015](#)). Our study showed that *CGR2* and *CGR3*, through pectin methylesterification, are capable of affecting total C assimilation by directly altering leaf area growth and by altering maintenance respiratory costs through direct effects on LMA. We also showed that although *CGR2* and *CGR3* affect area-based photosynthetic rates, the latter is not a major factor affecting overall plant growth.

A reduction in pectin methylesterification by reduced expression of *CGR2* and *CGR3* seems to enhance cell-wall

hardening and cell-to-cell adhesion through increased cross linking between GalUA and Ca^{2+} , favoring an increase in [LMA](#) against cell expansion and posing a greater demand for C for [LMA](#) growth compared to area growth ([Fig. 12A](#)). Hence less C will be utilized in area growth of new leaves and more C will be utilized in increasing [LMA](#), leading to a smaller projected leaf area ([Fig. 12A](#)). Smaller projected leaf area yields lower whole plant C assimilation. In contrast, an increase in pectin methylesterification via enhanced expression of *CGR2* and *CGR3* seems to reduce cell wall hardening and cell-to-cell adhesion, and thereby favors cell expansion and area growth against increases in [LMA](#); it poses a greater demand for C for leaf area growth compared to that for [LMA](#) growth ([Fig. 12B](#)). Hence, more C will be utilized in area growth of new leaves, and a lower proportion C will be utilized in [LMA](#) growth, leading to larger projected leaf area and enhanced whole-plant C assimilation ([Fig. 12B](#)). Suppression of *CGR2* and *CGR3* increases respiratory costs through higher [LMA](#), resulting in lower photosynthesis/respiration ratio, lower daily C gain, reduced net assimilated C available for growth, and ultimately reduced plant growth ([Fig. 12A](#)); over-expression of *CGR2* yields opposite physiological effects ([Fig. 12B](#)).

Figure 12.



[Open in a new tab](#)

CGR2- and *CGR3*-mediated pectin methylesterification regulates the relationship between photosynthesis and plant growth. A schematic diagram outlining how (A) suppression or (B) over-expression of *CGR2* and *CGR3* gene expression affects the relationship between photosynthesis and plant growth in Arabidopsis is presented. Suppression of *CGR2* and *CGR3* reduces the degree of pectin methylation, which leads to an increase in cell-to-cell adhesion, cation-mediated cross linking of GalUA, and consequent hardening of cell walls. *CGR2* over-expression increases the degree of pectin methylation, which allows cell expansion through reduced cell-to-cell adhesion and cation-mediated cross linking. We propose that pectin methyltransferase enzyme, through its ability to directly alter cell expansion, determines the amount of C partitioned to leaf area growth versus growth in terms of [LMA](#). For example, while more C is partitioned to growth in terms of [LMA](#) in the *CGR2* and *CGR3* double knockout mutant, in the *CGR2* over-expression line more C is partitioned to leaf area growth. An increase in [LMA](#) leads to enhanced area-based respiration and a reduction in leaf area contribute to a reduction in whole plant photosynthesis. Collectively, this results in a reduction in C available for growth

and consequently a decrease in overall plant growth; an opposite trend is seen in *CGR2OX*. Thus, *CGR2* and *CGR3*, through their ability to alter the degree of methylated pectin in the cell wall of the mesophyll cells, determine how photosynthate is utilized to grow the plant. In other words, *CGR2*- and *CGR3*-mediated pectin methylesterification affects the relationship between photosynthesis and plant growth by regulating the proportions of C that is partitioned to leaf area growth and [LMA](#). Final overall growth mainly depends on the expression patterns of *CGR2* and *CGR3* and how much C is partitioned to area growth and [LMA](#) and not on area-based photosynthesis. PME: pectin methylesterase; PMEI: PME inhibitor; PMT: pectin methyltransferase. CH₃OH is methanol.

There may be other genes that also impact partitioning of carbon toward leaf area growth or [LMA](#). One example is the xyloglucan endotransglucosylase/hydrolase (*XTH*) gene family. Reduced expression of *XTH8* and *XTH31* gene expression led to reduced leaf width, length, and leaf area ([Miura and Hasegawa, 2010](#)). The leaf mesophyll of these mutant lines consisted of a large number of small mesophyll cells per unit area ([Miura and Hasegawa, 2010](#)). Suppression of *XTH21* led to a reduction in cellulose, and xyloglucan content with subsequent reductions in both leaf and plant size ([Liu et al., 2007](#)). One of the major roles of XTH enzymes is cleavage of cross linkages between cellulose and hemicellulose microfibrils that promotes wall loosening and cell expansion. This may explain the above leaf phenotypes in *xth8*, *xth21*, and *xth31* mutant lines ([Liu et al., 2007](#); [Miura and Hasegawa, 2010](#)). Thus, through its effects on cell wall properties, *XTH* genes may be able to alter C partitioning to leaf area and LMA and thereby affect overall plant growth similar to the role played by *CGR* genes.

In summary, the results from this study are in agreement with findings from [Weraduwaage et al. \(2015\)](#) that optimization of leaf area growth and plant growth can be achieved by increased partitioning of C to leaf area growth with concomitant reduction in partitioning to growth in terms of [LMA](#) especially during the early vegetative growth phase ([Weraduwaage et al., 2015](#)), and that photosynthesis drives growth through alterations in C partitioning to leaf area and [LMA](#) growth. In this study, we found that *CGR2* and *CGR3* directly affect this relationship by altering the degree of cell expansion and/or adhesion, thereby driving C partitioning by generating C demands for leaf area growth and for growth in terms of [LMA](#).

CONCLUSION

Our study supports the model that qualitative and quantitative changes in pectin in the cell wall have a significant impact on area-based photosynthesis and respiration through alterations in leaf thickness, mesophyll cell density, and area of the leaf blade. Such changes in mesophyll architecture directly altered [LMA](#) and consequently area-based respiration. *CGR2* and *CGR3* affected area-based photosynthesis by altering CO₂ availability at Rubisco. These genes could affect plant-based photosynthesis by enabling enhanced light capture through larger leaf area. These data emphasizes the importance of pectin methylesterification in fine-tuning cell expansion and size, and adhesion qualities

when building an optimum leaf to maximize photosynthesis under different environmental conditions. While thin leaves are associated with reduced [LMA](#), it is important to maintain an optimum thickness to maintain sufficient intercellular air spaces that would maintain high internal conductance as reflected in S_{mes} and S_c and therefore higher carboxylation rates. *CGR2* and *CGR3*, which directly alter the size of the leaf blade and mesophyll architecture, may find applications in the future to improve light interception in crop plant canopies.

Over-expression of *CGR2* had a significant positive effect on leaf area and plant growth. Suppression of *CGR2* and *CGR3* caused a marked increase in [LMA](#), and a reduction in leaf area and plant growth. These differences resulted through changes in C partitioning to leaf area growth and growth in terms of [LMA](#) and not as a result of altered area-based photosynthesis rates. Therefore, photosynthesis drives plant growth through alterations in C partitioning to new leaf area growth and [LMA](#) growth, and this study discovered that pectin methylesterification affects this relationship by directly altering the degree of cell expansion and positioning in the leaves to create dynamic carbon demands in leaf area growth and leaf mass thereby driving C partitioning for these processes. Collectively, these results uncover an unexpected connection between cell wall composition and photosynthesis, and support the novel (to our knowledge) model that through its role in modulation of organ development, the cell wall plasticity is a key factor influencing photosynthetic processes in land plants.

MATERIALS AND METHODS

Growth Analysis

Wild-type *Arabidopsis* (Col-0), *cgr2/3* (loss of function double mutant line of *CGR2* and *CGR3*), *CGR2OX* (*CGR2* over-expression line), and *cgr2com* (*cgr2/3* complemented by *CGR2*) ([Kim et al., 2015](#)) were used in the study. Gene accession numbers for *CGR2* and *CGR3* are At3g49720 and At5g65810, respectively. Plants were grown hydroponically in 1/2-strength Hoagland's solution under a light intensity of $120 \mu\text{mol m}^{-2} \text{s}^{-1}$, using 8-h photoperiods with respective day- and night-time temperatures of 22°C and 20°C, and 60% relative humidity. The hydroponics system was housed in a model no. GC-20 Bigfoot Series Growth Chamber (BioChambers, Winnipeg, Manitoba, Canada).

Plant growth parameters including projected and total leaf area, leaf, root, and inflorescence dry weights, relative growth rates, specific leaf area ([SLA](#)), leaf mass per unit leaf area ([LMA](#)), leaf area ratio, and leaf, root, and inflorescence mass ratios were measured as described in [Weraduwage et al. \(2015\)](#). When calculating [SLA](#), [LMA](#), leaf area ratio, and leaf, root, and inflorescence mass ratios, the total leaf area, and organ and plant mass corresponding to each harvest was used: [SLA](#) ($\text{m}^2 \text{kg}^{-1}$) = total leaf area/leaf mass; [LMA](#) (kg m^{-2}) = leaf mass/total leaf area; leaf area ratio ($\text{m}^2 \text{kg}^{-1}$) = total leaf area/total plant mass; and leaf, root or inflorescence mass ratio (g g^{-1}) = leaf, root, or inflorescence mass/total plant mass. Growth measurements were obtained throughout the lifecycle of the plant at 2–3-

week intervals at 29, 49, 63, and 82 d after seeding ([DAS](#)). The 100-seed weight prior to stratification and sowing, cotyledon area, and hypocotyl length was also measured.

Determination of Leaf Thickness, Mesophyll Cell Density, S_{mes} , S_{c} , and Chloroplast Size and Abundance

Leaves of similar age from 34- and 51-d-old rosettes were used for anatomical measurements. Leaves were harvested and processed for leaf cross sectioning as described in [Weraduwaage et al. \(2015\)](#), at the Center for Advanced Microscopy, Michigan State University. Thin (500-nm) leaf sections (PTXL Ultramicrotome; RMC Boeckeler Instruments, Tucson, AZ) were observed under a SpectralView FV1000 Confocal Laser Scanning Microscope (Olympus, Melville, NY), and the distance between the adaxial and abaxial leaf surfaces was measured to determine leaf thickness.

Micrographs of leaf cross sections were used to determine the number of palisade and spongy parenchyma cells, the total number of cells, and the number of mesophyll cell layers in a 20,000 μm^2 area of a leaf cross section. These data were later expressed per mm^2 . ImageJ (<http://imagej.nih.gov/ij/>) software was utilized to measure the total area of intercellular air spaces, total length of mesophyll cells, total length of mesophyll cells exposed to intercellular air spaces (L_{mes}), and the total length of chloroplasts exposed to intercellular air spaces (L_{c}). The latter three measurements were utilized to determine the surface area of mesophyll cells exposed to intercellular air spaces (S_{mes}) and the surface area of chloroplast exposed to intercellular air spaces (S_{c}) per unit leaf area as described in [Evans et al. \(1994\)](#).

A series of z-stack images of leaves of 34-d-old plants was acquired using an inverted laser scanning confocal microscope (model no. LSM510 META, Carl Zeiss; <http://www.zeiss.com>). Chloroplasts were imaged using an ECPlan-Neofluar 40 \times /1.30 oil M27 objective (Carl Zeiss) at a 512 \times 512 pixel resolution using an excitation wavelength of 514 nm and an emission wavelength of 673 nm. The different planes acquired were then projected on the same image and transformed in binary using Image J. The resulting number of chloroplasts per unit area and average chloroplast size was also measured using ImageJ.

Gas Exchange Measurements, $^{14}\text{CO}_2$ Feeding Experiments, and Analysis of Leaf ^{13}C Discrimination

Whole rosette photosynthesis and nighttime dark respiration were measured at 2–3 week intervals at 29, 49, 63, and 82 [DAS](#). A custom-built rosette-gas-exchange chamber connected to a model no. LI-6400 portable gas exchange system (LI-COR Biosciences, Lincoln, NE) was used to obtain photosynthesis and respiratory measurements. Conditions in the Arabidopsis rosette gas-exchange chamber during photosynthesis measurements were: a leaf temperature of 22°C; $[\text{CO}_2]$ of 400 $\mu\text{mol mol}^{-1}$; and 120 $\mu\text{mol m}^{-2} \text{s}^{-1}$ light intensity. During night-time respiration measurements, the leaf

temperature was maintained at 20°C. Flow rate was set at 500 $\mu\text{mol s}^{-1}$ when making measurements from 49- and 63-d-old plants. For 29- and 82-d-old plants, flow rate was set at 300 and 700 $\mu\text{mol s}^{-1}$, respectively, to better control humidity.

After the initial measurements of photosynthesis, 29-d-old Arabidopsis rosettes were fed with $^{14}\text{CO}_2$ for 10 min. After a 2-h chase period, leaf and root tissue were harvested separately into scintillation vials. Radioactivity was determined as disintegrations per min (**DPM**) by liquid scintillation counting. The **DPM** values recorded from roots and rosettes and the total **DPM** were used to calculate the proportion of C present in these organs.

The content ratio of $^{13}\text{CO}_2$ to $^{12}\text{CO}_2$ in Arabidopsis freeze-dried leaf material was measured at the Stable Isotope Ratio Facility for Environmental Research, University of Utah (Salt Lake City, UT), by mass spectrometry. These data were used to calculate the $\delta^{13}\text{C}_{\text{VPDB}}$ value, which is the ^{13}C to ^{12}C isotopic ratio of leaves relative to the ^{13}C to ^{12}C isotopic ratio of the Vienna-Pee-Dee Belemnite (**VPDB**) standard ([Farquhar et al., 1982](#)). The $\delta^{13}\text{C}_{\text{VPDB}}$ values were used to calculate the CO_2 partial pressure at Rubisco using Eq. 12 given in [Farquhar et al. \(1982\)](#). Values for the various factors are as follows: δ -value of CO_2 in the air at present = -8.4‰ (<http://www.esrl.noaa.gov>); partial pressure of CO_2 in the air = 39 Pa; ^{13}C discrimination associated with the diffusion of CO_2 through air = 4.4‰ ; and ^{13}C discrimination in the carboxylation reaction = 27‰ ([Farquhar et al., 1989](#)).

Analysis of Cell Wall Polysaccharides in Leaves

Preparation of alcohol-insoluble residues and uronic acid and methyl ester assays were performed based on the methodology described in [Kim et al. \(2015\)](#). The matrix polysaccharide (hemicellulose) and crystalline cellulose composition, and soluble sugar content in leaves, were measured at the Great Lakes Bioenergy Research Center Cell Wall Facility, Michigan State University (East Lansing, MI) as described in [Kim et al. \(2015\)](#).

Parameterization of the Arabidopsis Leaf Area Growth Model

Development, parameterization, and execution of the Arabidopsis leaf area growth model were described in detail in [Weraduwaage et al. \(2015\)](#). This model is a tool to determine partitioning coefficients of C that could give rise to the growth patterns observed in different plants ([Weraduwaage et al., 2015](#)). In the model, plant growth is divided into four growth stages: (1) heterotrophic phase (1–4 **DAS**); (2) early vegetative phase; (3) late vegetative phase; and the (4) reproductive phase. Ninety days of plant growth are simulated in the model using a fixed time step of 1 h and the photoperiod is set at 8 h. As described in detail in [Weraduwaage et al. \(2015\)](#), the following were used as inputs of the model: weight of storage reserves, ratio of mobilized storage reserves to stored reserves, initial leaf area, initial leaf mass, projected to total leaf area ratio, net photosynthesis rate per unit leaf area, proportion of C stored as starch during the day, leaf maintenance and growth respiratory coefficients, photoperiod, and lengths of growth phases.

Values for area-based photosynthesis obtained during the four harvests were fitted with a polynomial third-order equation to extrapolate area-based photosynthesis through the entire 90 d of the lifecycle. Similarly, measured projected to total leaf area ratios during the four harvests were fitted with a polynomial second-order equation to extrapolate the values over 90 d. These extrapolated values were used in the model as input photosynthesis values and projected to total leaf area ratios over the life span. The model also takes both growth and maintenance respiration into consideration. The model considers maintenance respiration of a plant/particular organ to be proportional to the corresponding dry mass and growth respiration to be proportional to the growth rate ([Penning de Vries et al., 1974](#); [Amthor, 1984](#); [Thomas et al., 1993](#); [Lambers et al., 2008](#)). The model has set values for maintenance coefficients (amount of C respired to maintain the existing mass of the plant or specific organ, $\mu\text{mol C g}^{-1} \text{ s}^{-1}$), and for growth coefficients (amount of C respired per unit increase in mass, g g^{-1}) based on values provided in the literature ([Amthor, 1984](#); [Mariko, 1988](#)) and assumes that growth respiration coefficients of leaf growth in terms of area and LMA are the same throughout the lifecycle. The net amount of C available for growth and maintenance processes of the plant is determined as the product of area-based photosynthetic rate and the projected leaf area. Next, C consumed in maintenance respiration and exudation is subtracted to determine the net assimilation rate, which provides the amount of C available for growth. The model then simulates the partitioning of C available for growth to leaf area growth, growth in terms of [LMA](#), and root and inflorescence growth based on the set partitioning coefficients that are adjustable to facilitate fitting of the data. Partitioning coefficients vary based on the growth phases. The increase in mass during growth in terms of leaf area and [LMA](#), and root and inflorescence growth, is calculated by subtracting the C consumed in growth respiration from the total C allocated for growth of that particular organ. Accordingly, the model simulates the increase in leaf area and mass, and the mass of the inflorescence and roots. The model calculated [SLA](#), [LMA](#), and leaf, root, and inflorescence mass ratios over time based on the equations given above.

To fit the modeled data to measured data, 16 partitioning coefficient parameters (partitioning to the inflorescence, roots, leaf area and [LMA](#), for each of the four growth phases: germination phase, early and late vegetative phases, and reproductive phase) were adjusted so that the modeled and measured leaf area, mass of inflorescence, root, and leaf matched ([Weraduwaage et al., 2015](#)). C partitioning data obtained by feeding Arabidopsis rosettes at 29 [DAS](#) with $^{14}\text{CO}_2$ were used as initial estimates that were fine-tuned to fit the data. Sensitivity of the model to changes in the inputs was tested in Col-0 by simulating an increase or decrease of 1% in C partitioned to growth processes, and other model inputs, and noting the resulting response in output. The model was considered sensitive, in cases where more than 1% variation occurred in model outputs because of changing a particular input.

Statistical Analyses of Experimental Data

Four to five biological replicates per line were used to collect experimental data at a given time point. Statistical analyses were carried out using SPSS 22 (IBM, Armonk, NY). The effects of altered *CGR2* and *CGR3* expression on plant growth and gas exchange were compared using a univariate general linear model and the differences between means were tested by subjecting data to one-way ANOVA at $\alpha = 0.05$, followed by a Fisher's Least Significant

Difference Test. Measured data presented in figures represent the mean \pm standard error (SE).

Accession Numbers

Sequence data from this article can be found in the GenBank/EMBL data libraries under accession numbers At3g49720 and At5g65810.

Supplemental Data

The following supplemental materials are available.

- [Supplemental Figure S1](#) . Cell wall composition in Arabidopsis with altered *CGR2* and *CGR3* expression.
- [Supplemental Figure S2](#) . Hypocotyl and rosette size in Arabidopsis with altered *CGR2* and *CGR3* expression.
- [Supplemental Figure S3](#) . Early growth phenotypes in Arabidopsis with altered *CGR2* and *CGR3* expression.
- [Supplemental Figure S4](#) . Partitioning of photosynthetic C to shoots and roots in Arabidopsis with altered *CGR2* and *CGR3* expression.

Supplementary Material

Supplemental Data

[supp_171_2_833_index.html](#) (1.5KB, html)

Acknowledgments

We are grateful to Drs. Sean E. Weise (Department of Biochemistry and Molecular Biology), Cliff Foster (the Cell Wall Facility, Great Lakes Bioenergy Research Center), Alicia Withrow and Melinda Frame (Center for Advanced Microscopy) of Michigan State University (East Lansing, MI), and Dr. Suvankar Chakraborty (Stable Isotope Ratio Facility for Environmental Research) of the University of Utah for their support. We thank Jim Klug and Cody Keilen (Growth Chamber Facility) of Michigan State University for their assistance and all members of the Sharkey and Brandizzi labs for their support.

Glossary

DAS

days after seeding

DPM

disintegrations per min

LMA

mass per unit leaf area

LMD

leaf mass density

SLA

specific leaf area

VPDB

Vienna-Pee-Dee Belemnite

Footnotes

¹Funding for this research was provided by the Chemical Sciences, Geosciences and Biosciences Division, Office of Basic Energy Sciences, Office of Science, U.S. Department of Energy (award no. DE-FG02-91ER20021) and in part by the Department of Energy Great Lakes Bioenergy Research Center (Department of Energy Office of Science no. BER DE-FC02-07ER64494). Partial salary support for T.D.S. and F.B. came from Michigan AgBioResearch.

[OPEN]Articles can be viewed without a subscription.

References

1. Amthor JS. (1984) The role of maintenance respiration in plant growth. *Plant Cell Environ* 7: 561–569 [[Google Scholar](#)]
2. Burton RA, Gibeaut DM, Bacic A, Findlay K, Roberts K, Hamilton A, Baulcombe DC, Fincher GB (2000) Virus-induced silencing of a plant cellulose synthase gene. *Plant Cell* 12: 691–706 [[DOI](#)] [[PMC free article](#)] [[PubMed](#)] [[Google Scholar](#)]
3. Caffall KH, Mohnen D (2009) The structure, function, and biosynthesis of plant cell wall pectic polysaccharides. *Carbohydr Res* 344: 1879–1900 [[DOI](#)] [[PubMed](#)] [[Google Scholar](#)]

4. Cunningham SA, Summerhayes B, Westoby M (1999) Evolutionary divergences in leaf structure and chemistry, comparing rainfall and soil nutrient gradients. *Ecol Monogr* 69: 569–588 [[Google Scholar](#)]
5. Evans JR, von Caemmerer S, Setchell BA, Hudson GS (1994) The relationship between CO₂ transfer conductance and leaf anatomy in transgenic tobacco with a reduced content of rubisco. *Aust J Plant Physiol* 21: 475–495 [[Google Scholar](#)]
6. Farquhar G, Ehleringer J, Hubick K (1989) Carbon isotope discrimination and photosynthesis. *Annu Rev Plant Physiol Plant Mol Biol* 40: 503–537 [[Google Scholar](#)]
7. Farquhar G, O’Leary M, Berry J (1982) On the relationship between carbon isotope discrimination and the intercellular carbon dioxide concentration in leaves. *Funct Plant Biol* 9: 121–137 [[Google Scholar](#)]
8. Galmés J, Ochogavía JM, Gago J, Roldán EJ, Cifre J, Conesa MÀ (2013) Leaf responses to drought stress in Mediterranean accessions of *Solanum lycopersicum*: anatomical adaptations in relation to gas exchange parameters. *Plant Cell Environ* 36: 920–935 [[DOI](#)] [[PubMed](#)] [[Google Scholar](#)]
9. Heldt H-W, Piechulla B (2010) *Plant Biochemistry*, Ed 4 Academic Press, London, UK [[Google Scholar](#)]
10. Honda H, Fisher JB (1978) Tree branch angle: maximizing effective leaf area. *Science* 199: 888–890 [[DOI](#)] [[PubMed](#)] [[Google Scholar](#)]
11. Kim HS, Delaney TP (2002) Over-expression of TGA5, which encodes a bZIP transcription factor that interacts with NIM1/NPR1, confers SAR-independent resistance in *Arabidopsis thaliana* to *Peronospora parasitica*. *Plant J* 32: 151–163 [[DOI](#)] [[PubMed](#)] [[Google Scholar](#)]
12. Kim S-J, Held MA, Zemelis S, Wilkerson C, Brandizzi F (2015) CGR2 and CGR3 have critical overlapping roles in pectin methylesterification and plant growth in *Arabidopsis thaliana*. *Plant J* 82: 208–220 [[DOI](#)] [[PubMed](#)] [[Google Scholar](#)]
13. Lambers H, Chapin F, Pons T (2008) *Plant Physiological Ecology*, Ed 2 Springer, New York, NY [[Google Scholar](#)]
14. Lionetti V, Raiola A, Camardella L, Giovane A, Obel N, Pauly M, Favaron F, Cervone F, Bellincampi D (2007) Overexpression of pectin methylesterase inhibitors in *Arabidopsis* restricts fungal infection by *Botrytis cinerea*. *Plant Physiol* 143: 1871–1880 [[DOI](#)] [[PMC free article](#)] [[PubMed](#)] [[Google Scholar](#)]
15. Liu YB, Lu SM, Zhang JF, Liu S, Lu YT (2007) A xyloglucan endotransglucosylase/hydrolase involves in growth of primary root and alters the deposition of cellulose in *Arabidopsis*. *Planta* 226: 1547–1560 [[DOI](#)] [[PubMed](#)] [[Google Scholar](#)]

16. Mariko S. (1988) Maintenance and constructive respiration in various organs of *Helianthus annuus* L. and *Zinnia elegans* L. Bot Mag 101: 73 [[Google Scholar](#)]
17. Mitchell KA, Bolstad PV, Vose JM (1999) Interspecific and environmentally induced variation in foliar dark respiration among eighteen southeastern deciduous tree species. Tree Physiol 19: 861–870 [[DOI](#)] [[PubMed](#)] [[Google Scholar](#)]
18. Miura K, Hasegawa PM (2010) Sumoylation and other ubiquitin-like post-translational modifications in plants. Trends Cell Biol 20: 223–232 [[DOI](#)] [[PubMed](#)] [[Google Scholar](#)]
19. Penning de Vries FW, Brunsting AHM, van Laar HH (1974) Products, requirements and efficiency of biosynthesis: a quantitative approach. J Theor Biol 45: 339–377 [[DOI](#)] [[PubMed](#)] [[Google Scholar](#)]
20. Pilling J, Willmitzer L, Bücking H, Fisahn J (2004) Inhibition of a ubiquitously expressed pectin methyl esterase in *Solanum tuberosum* L. affects plant growth, leaf growth polarity, and ion partitioning. Planta 219: 32–40 [[DOI](#)] [[PubMed](#)] [[Google Scholar](#)]
21. Poorter H, Niinemets U, Poorter L, Wright IJ, Villar R (2009) Causes and consequences of variation in leaf mass per area (LMA): a meta-analysis. New Phytol 182: 565–588 [[DOI](#)] [[PubMed](#)] [[Google Scholar](#)]
22. Shipley B. (2002) Trade-offs between net assimilation rate and specific leaf area in determining relative growth rate: relationship with daily irradiance. Funct Ecol 16: 682–689 [[Google Scholar](#)]
23. Terashima I, Hanba YT, Tazoe Y, Vyas P, Yano S (2006) Irradiance and phenotype: comparative eco-development of sun and shade leaves in relation to photosynthetic CO₂ diffusion. J Exp Bot 57: 343–354 [[DOI](#)] [[PubMed](#)] [[Google Scholar](#)]
24. Thomas RB, Reid CD, Ybema R, Strain BR (1993) Growth and maintenance components of leaf respiration of cotton grown in elevated carbon dioxide partial pressure. Plant Cell Environ 16: 539–546 [[Google Scholar](#)]
25. Tsuge T, Tsukaya H, Uchimiya H (1996) Two independent and polarized processes of cell elongation regulate leaf blade expansion in *Arabidopsis thaliana* (L.) Heynh. Development 122: 1589–1600 [[DOI](#)] [[PubMed](#)] [[Google Scholar](#)]
26. Villar R, Ruiz-Robledo J, Ubera JL, Poorter H (2013) Exploring variation in leaf mass per area (LMA) from leaf to cell: an anatomical analysis of 26 woody species. Am J Bot 100: 1969–1980 [[DOI](#)] [[PubMed](#)] [[Google Scholar](#)]
27. Weraduwege SM, Chen J, Anozie FC, Morales A, Weise SE, Sharkey TD (2015) The relationship between leaf area growth and biomass accumulation in *Arabidopsis thaliana*. Front Plant Sci 6: 167. [[DOI](#)]

[\[PMC free article\]](#) [\[PubMed\]](#) [\[Google Scholar\]](#)]

28. Witkowski ETF, Lamont B (1991) Leaf specific mass confounds leaf density and thickness. *Oecologia* 88: 486–493 [\[DOI\]](#)] [\[PubMed\]](#) [\[Google Scholar\]](#)]
29. Wolf S, Mouille G, Pelloux J (2009) Homogalacturonan methyl-esterification and plant development. *Mol Plant* 2: 851–860 [\[DOI\]](#)] [\[PubMed\]](#) [\[Google Scholar\]](#)]
30. Xiao C, Anderson CT (2013) Roles of pectin in biomass yield and processing for biofuels. *Front Plant Sci* 4: 67. [\[DOI\]](#)] [\[PMC free article\]](#) [\[PubMed\]](#) [\[Google Scholar\]](#)]

Associated Data

This section collects any data citations, data availability statements, or supplementary materials included in this article.

Supplementary Materials

Supplemental Data

[supp_171_2_833_index.html](#) (1.5KB, html)

[supp_pp.16.00173_PP2016-00173R1_Supplemental_Materialfig1.pdf](#) (258.7KB, pdf)

[supp_pp.16.00173_PP2016-00173R1_Supplemental_Materialfig2.pdf](#) (260.9KB, pdf)

[supp_pp.16.00173_PP2016-00173R1_Supplemental_Materialfig3.pdf](#) (186.1KB, pdf)

[supp_pp.16.00173_PP2016-00173R1_Supplemental_Materialfig4.pdf](#) (192.9KB, pdf)